NREL
NATIONAL RENEWABLE ENERGY LABORATORY

An End of Service Life Assessment of PMMA Lenses from Veteran Concentrator Photovoltaic Systems

David C. Miller[1], Hussameldin I. Khonkar[2], Rebeca Herrero[3], Ignacio Antón[3], David K. Johnson[4], Todd B. Vinzant[4], Steve Deutch[4], Bobby To[1], Gabriel Sala[3], and Sarah R. Kurtz[1]

[1] National Center for Photovoltaics, National Renewable Energy Laboratory, (NREL) Golden, CO, USA
[2] Water and Energy Research Institute, King Abdulaziz City for Science and Technology (KACST), Riyadh, Saudi Arabia
[3] Instituto de Energía Solar - Universidad Politécnica de Madrid (IES-UPM), Madrid, Spain
[4] Biosciences Center, NREL, Golden, CO, USA

*Presenter, David.Miller@nrel.gov

2015 International Conference on Concentrator Photovoltaics ("CPV-11")

Auditorium, Aix-les-Bains Congress Center, Aix-les-Bains, France

14:00 (15 min) Weds, 2015/4/15

NREL/PR-5J00-67733

History of the SolERAS Program & the "Solar Village" Site

- Solar Energy Research American Saudi (1977) built the world's first large CPV system to power 3 then rural villages of Al-Hajrah, Al-Uyaynah, and Al-Jubaiah.
- Includes 350 kW of Martin-Marietta CPV modules, 1.6MHw Lead-acid batteries, and four 250 KVA standby diesel generators.
- Commissioned as stand alone power plant in Nov, 1981; connected to the national grid in Sept. 1984.
- Site incorporated into KACST (Riyadh) in 1986.

≥20 years successful operation:

- The most veteran CPV system in the world.
- Benchmark CPV location in Saudi desert.
- History includes a variety of operating configurations.
- Similar 225 kW M-M system installed in Phoenix, April 1982.

Photograph of the SolERAS site.
See also: Bowen, *Proc PLEA Conf.*, 1985.

Salim and Eugenio, *SOLMAT*, 29, 1990, 1-24.
Salim et. al., *Proc. IEEE PVSC*, 1987, 1351-1357.

Details of the Martin-Marietta CPV Technology

- C_g =36.5x, using PMMA lens. *f*/1.4 (nominal).
- Lens: 30.5 cm x 30.5 cm size; 4.5 mm thickness

35.978 cm/42.672 cm operating/focal distances.

- Si cell with circular gridline design.
- 4 lens parquet, with 64 parquets/tracker.

160 trackers → 10,240 lenses in system.

- SolERAS modules were cleaned using pressurized DI water monthly (first 3 years), then quarterly after connected to the grid.

Modules automatically stowed (face-down) from sunset to sunrise; also on rainy days, and during dust storms.

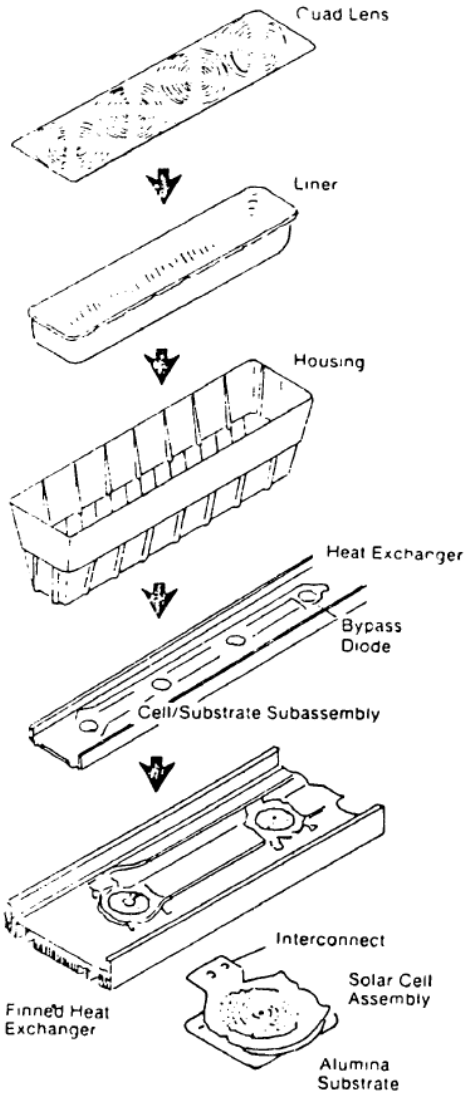

Schematic showing components of the M-M CPV design. McGuirk, DOE/ET/20624-1, 1984, pp 1-60.

Details of the Martin-Marietta CPV Technology

- Module body consists of plastic housing (not PMMA).

- Discoloration (lens entirely yellow) for ~2% lenses. Originally attributed to UV stabilizer, later to adhesive.

- Discoloration (and delamination) resolved using a replacement (silicone) adhesive.

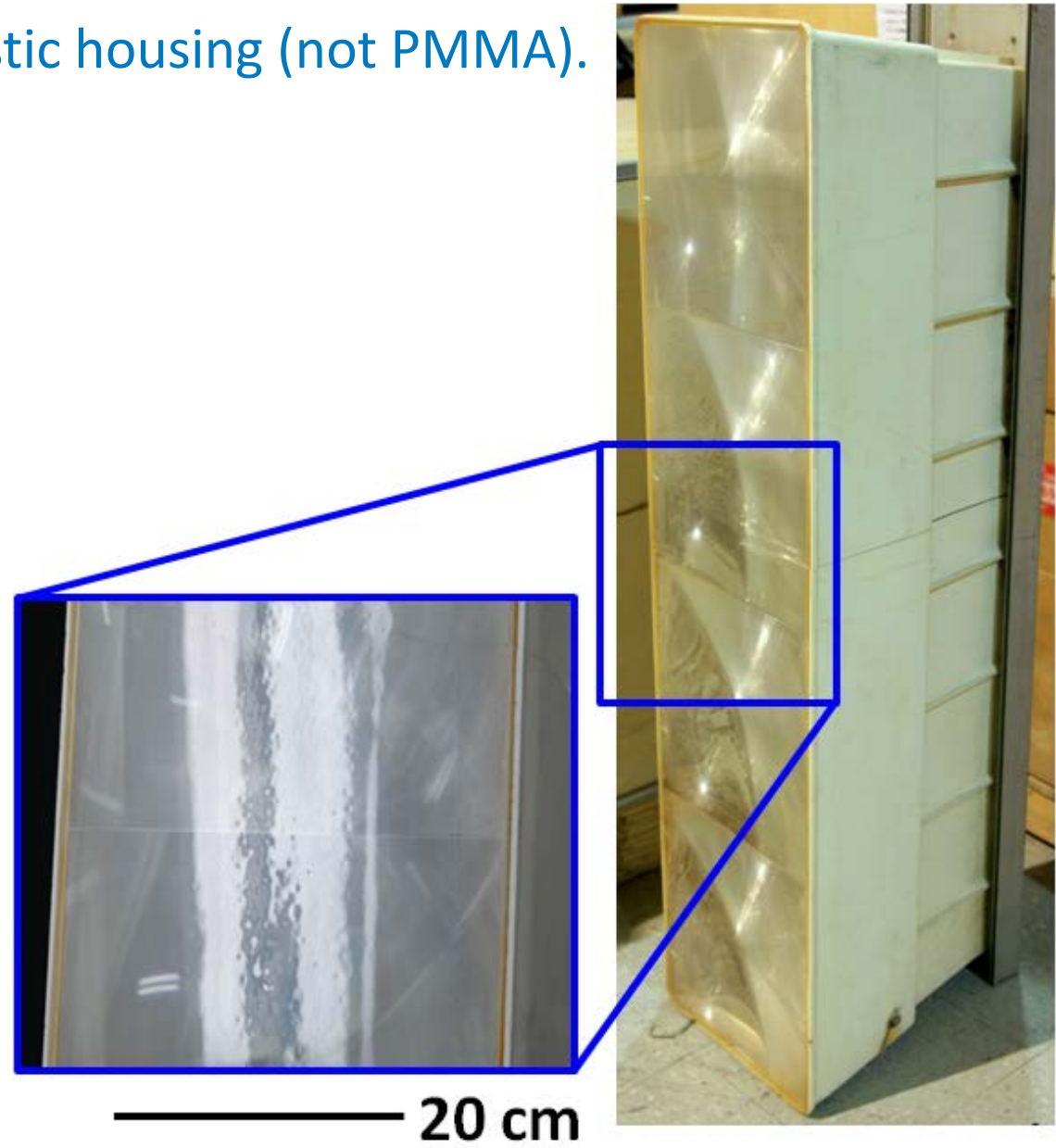

Photographs of M-M module (NREL warehouse), revealing the dimpled surface of the lens.

Goals & Experiments for Veteran Lens Characterization

- 33 year old samples are reliability-research treasure!
- Use SolERAS (Riyadh) veteran lenses as example in this presentation.
  - "Field" samples (tracking for 20 years).
  - Reference samples (KACST: stacked outdoors; NREL: warehouse).

Goals:

- Quantify performance of M-M lenses after >30 years of field aging.
- Identify significant degradation modes.

EXAMINATION	EQUIPMENT	SITE
lens performance with PV device (MJ or SI)	solar simulator	IES-UPM
material optical transmittance	spectrophotometer	NCPV-NREL
material integrity (molecular weight)	gel permeation chromatography	BSC-NREL
surface roughness	SEM & AFM	NCPV-NREL
active electronic structure	UV-VIS fluorescence spectroscopy	NCPV-NREL
chemical content	gas chromatography-mass spectroscopy	BSC-NREL

Summary of the characterizations performed.
Green: presented today.
Red: auxiliary measurements

Lens Measurements (CPV Solar Simulator at UPM)

- Use Si or MJ solar cell (A_{MJ}=1cm^2) for measuring E_{out} (irradiance at lens exit).
- Use isotype cells for measuring E_{in} (irradiance at lens entrance) for spectral effects.

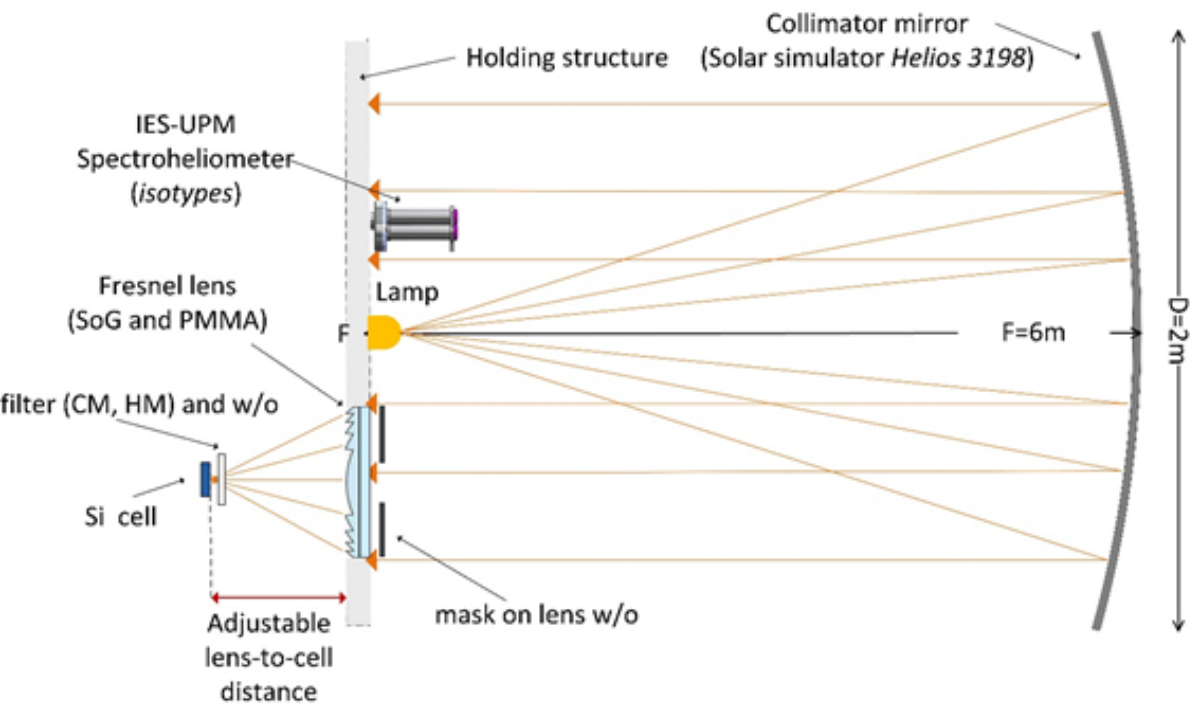

Schematic: use of UPM CPV Solar Simulator with veteran lens.
Domínguez et. al., Optics Express, 16 (19), 2008, 14894–14901, 2008.

$$\eta = \frac{E_{out} \cdot A_{cell}}{E_{in} \cdot A_{lens}}$$

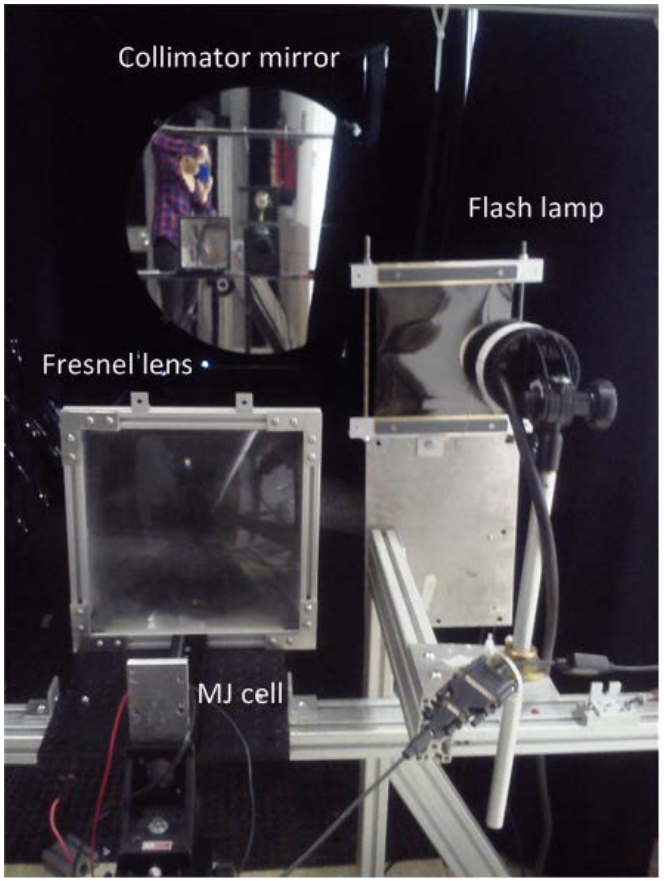

Photo: Implementation with M-M lens.

- Spectrum for light pulses from solar simulator varies with time.

⇒Use Spectral Matching Ratio (SMR) to quantify the color cast of the light during characterization.

Lens Results: Measurements Comparing Lenses

- Each lens first aligned with test cell at focal distance of 400mm.
- SMR=1±2% (relative to AM1.5 direct) at 900W·m^{-2}
- η_o= 87.5% for Riyadh, where $\eta_o = \eta_{field}/\eta_{reference}$.
- Lens curvature ⇒distinct optimum focal distances observed for each lens!
- Loss from κ & lens design would be increased in module (lenses not aligned individually).
- Data suggests optical loss ($\Delta\tau$) in addition to change in focal length.

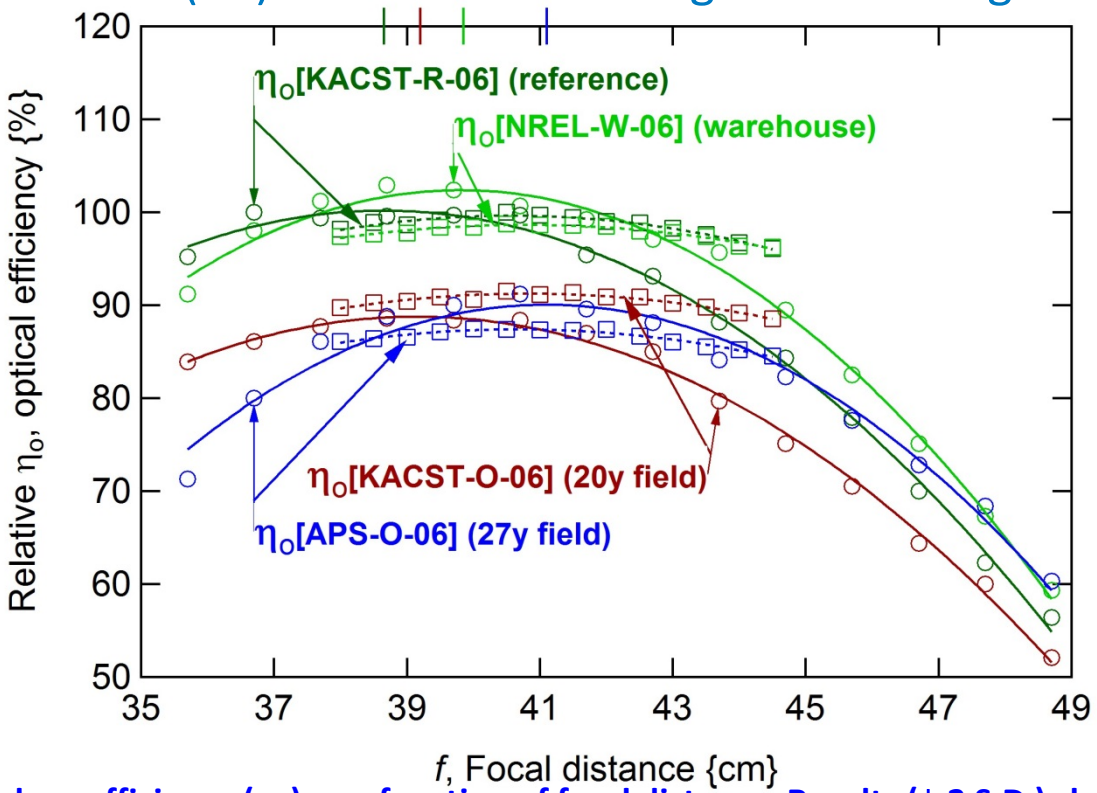

Comparison of relative lens efficiency (η_o) as a function of focal distance. Results (± 2 S.D.) shown for Si cell. Scans for the entire lens are indicated using a circle with best fits using solid lines; scans for the lens center (8 cm x 8 cm mask) are shown using squares and dashed lines. For the measurements of the entire lens, hash-marks shown at top for optimal η_o.

Material Spectral Bandwidth Minimally Affected

- Veteran and reference **lenses** examined with integrating sphere.
- λ_{cUV} of: 373→375 nm. Suggests UV stabilization still present.
- *YI* of: 1.33→1.59. Implies minimal chromophore formation. Yellowness not visually observed.
- *Spectral bandwidth, λ_{cUV}, and* YI *cannot account for the loss in lens performance.*

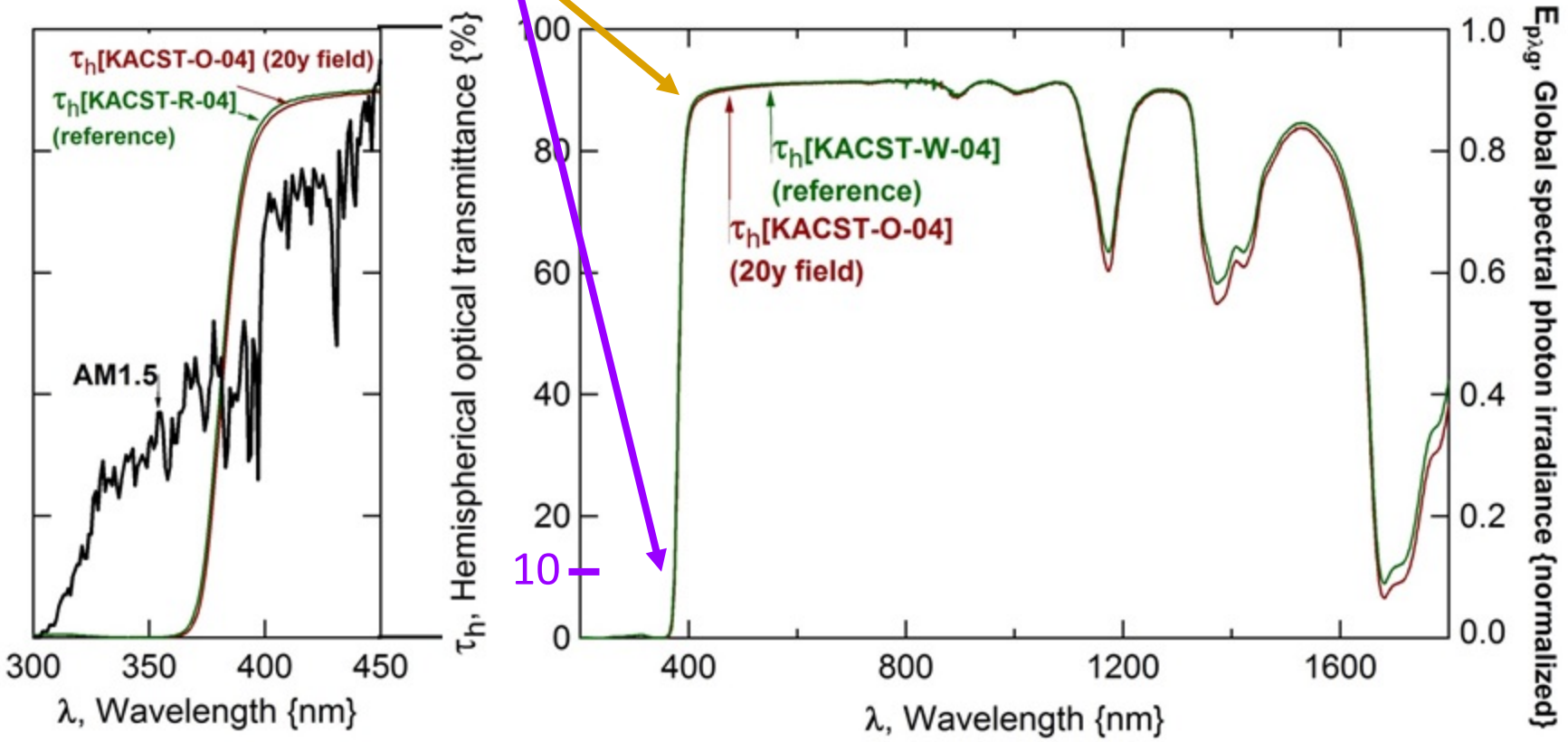

Spectral transmittance for veteran lens KACST-O-04 (fielded 20 years in Riyadh) and the reference lens KACST-R-04 (stored in stack outside). The UV transmittance is compared to the AM1.5D spectral photon irradiance in the inset (left).

Minor UV Damage is Evident From the M_w

- UV photodegradation of PMMA occurs via random chain scission.

Miller and Kurtz, SOLMAT, 95 (8), 2011, 2037-2068. (DOI:10.1016/j.solmat.2011.01.031)

- A decrease in M_w is seen for the front surface, consistent with the literature.
- Distribution of M_w is not changed, suggesting –*random*- scission.
- Compared to previous slide: the ΔM_w for front surface does not greatly affect material τ.
- ΔM_w might mechanically contribute to a through-thickness strain gradient (facilitating Δ curvature).
- $\Delta M_w \Rightarrow K_{IC}\downarrow$: might facilitate surface–crazing or –erosion.

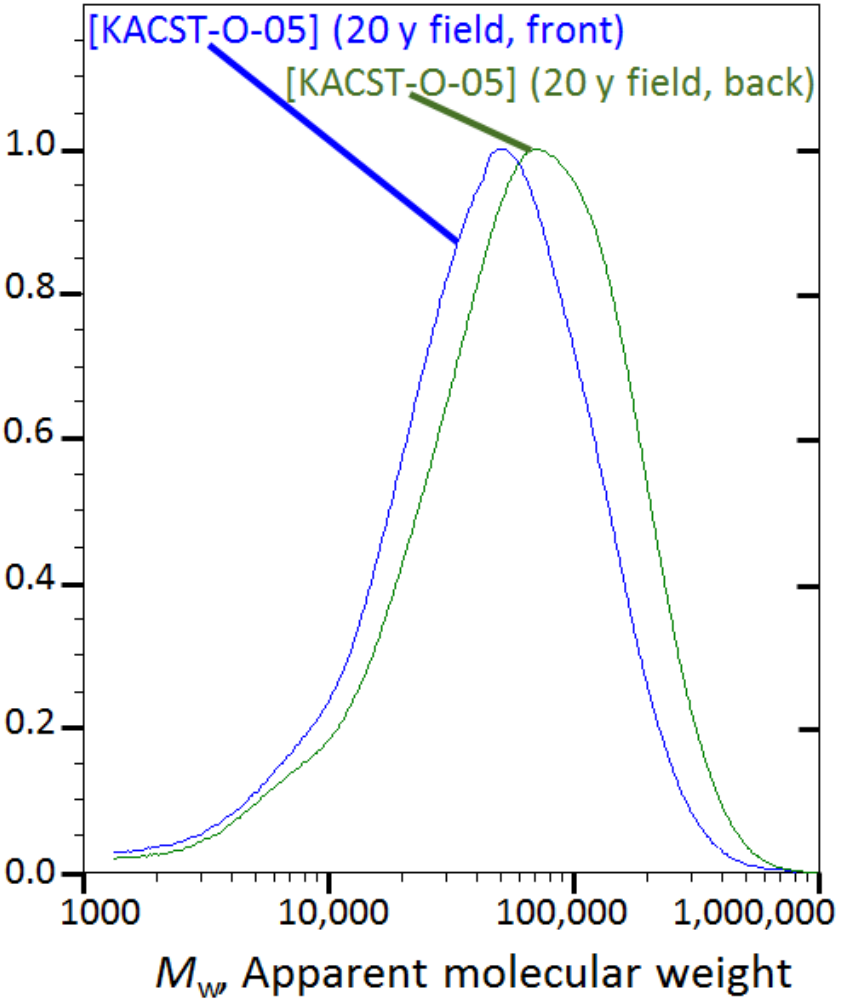

Molecular weight for veteran lens KACST-O-05 (fielded 20 years in Riyadh). Data (≤ 100 μm sample depth) is shown for the first surface, facing the environment "front" as well as the surface facing the module interior "back".

Modest Haze Observed in Material Transmittance

- Portions of lens measured: (1) as-received, (2) after milling and polishing back surface, and (3) after polishing front (field) surface.
- ~1% transmittance difference (τ_{sw}) for facets.
- ~0.2% difference when front surface is polished.
- Front polish: haze follows from field use.
- *Presently studying how much haze (abrasion or erosion) of the first surface affects lens performance.*

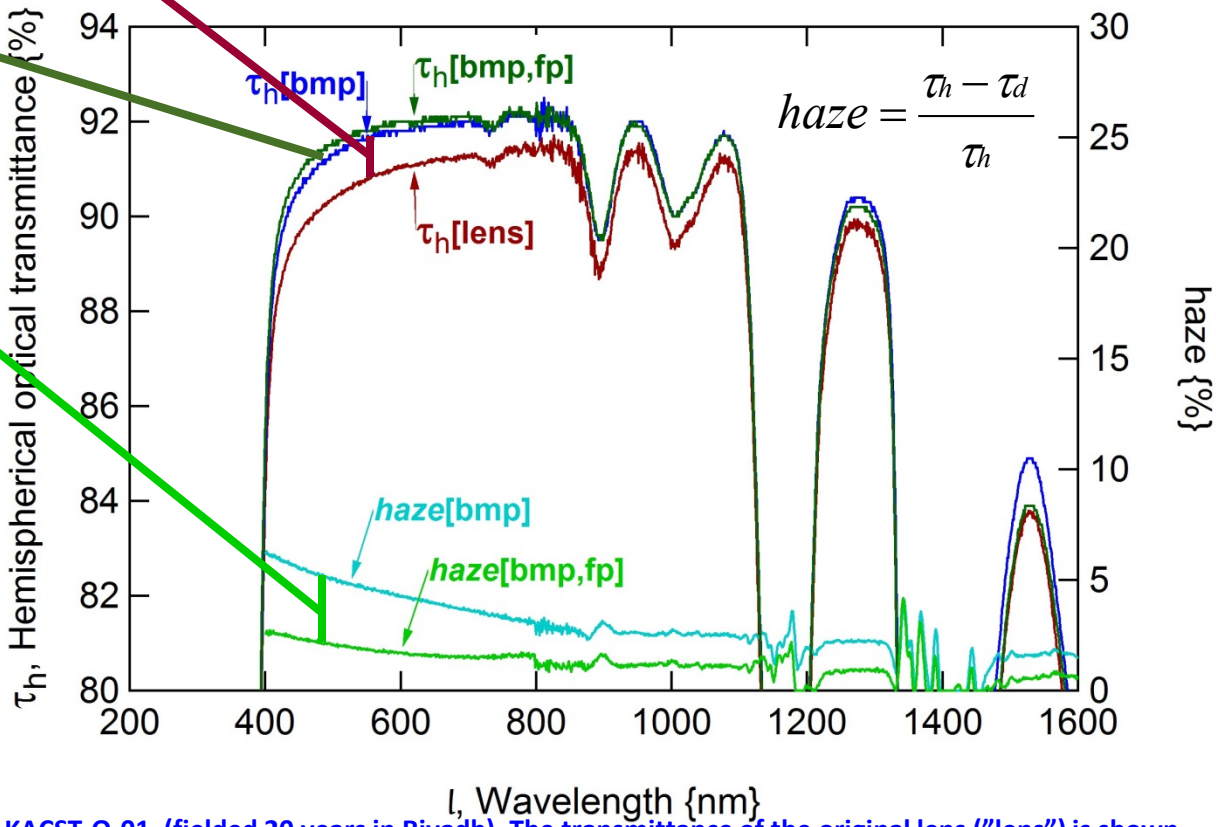

Spectral transmittance and optical haze for veteran lens KACST-O-01 (fielded 20 years in Riyadh). The transmittance of the original lens ("lens") is shown relative to the same lens with the faceted back surface milled and polished ("bmp"), and then subsequently polished on the front ("bmp,fp"). Measurements for the polished samples have been compensated to the nominal lens thickness of 4.51 mm. *Haze* is determined as the percent difference in the hemispherical and direct transmittance.

Lens Curvature is Significant

- No object is perfectly flat. Radius of curvature can be estimated from the measured deflection relative to the specimen size.
- R=0.5 m in example.
- Lenses from other locations & history also curved.
- κ is overt here.

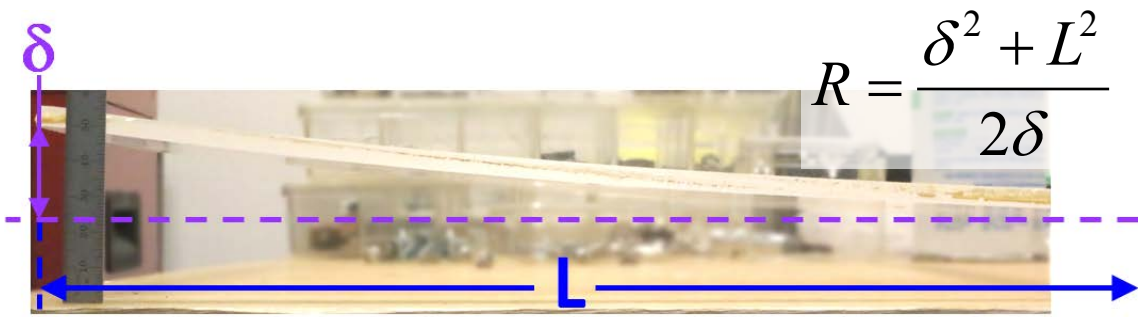

Photograph (side view) of parquet removed from module. Image shown for NREL warehouse specimen.

Enabling factors:

- Gravity and wind sag.
- Residual stress from manufacture.

(Facets make lens asymmetric about neutral axis.)

- T_α (T_g) of PMMA ~105 °C.

(Softening and physical aging.)

Solutions (to reduce curvature):

- Low stress manufacture process.
- Design: smaller lens area, or thicker lens/parquet.
- Attachment scheme: adhesive choice & strain relieving design.
- Secondary optical element.

Summary & Conclusions.

- Optical- & materials-characterization performed on PMMA lenses from veteran CPV sites, including the Saudi SolERAS site near Riyadh.
- Loss in η_o of ~10% observed for some lenses.

- Most significant optical loss observed from optical scattering.
- Scattering follows from the roughness of the first surface, not a change in the radius of the prism tip or valley.
- Natural abrasion and/or lasting contamination of the first surface are implied here from atomic force and electron microscopy.
- Lens curvature was observed, but its optical effect was not significant.

- ΔYI and $\Delta\lambda_{cUV} \rightarrow 0$. Discoloration (optical absorption) not significant.
- No microscopic evidence crazing or cracking. $M_w >$ embrittlement threshold.

- Additional $\Delta\ \eta_o$ from voids in surface of APS M-M lenses.
- Voids may result from solvent interactions (Phoenix Sky Harbor airport).

Acknowledgements

- NREL: Dr. Jeffrey Blackburn, Dr. James Burst, Dr. Mike Kempe, Dr. Matthew Gray, Dr. Daryl Myers, Dr. John Pern, Kate Baughman, Greg Perrin, Ian Tappan.
- KACST Saudi National Research Center: F.M. Al-Alweet, A. Alyahya, N. Eugenio, M. Halawani, A. Al Owais.
- Fraunhofer ISE: Peter Jakob.
- Arizona Public Service, S.T.A.R. Center: Howard Barikmo, Tom Lepley, Michael Longyear, Joe McGuirk, Scott Steele, and John Wiedner.
- Martin-Marietta Corp.: Sidney Broadbent, David Hughes.
- Sandia National Laboratories: Eldon Boes, Mike Edenburn, Olga Lavrova, and Charlie Stillwell.

- See also Arndt *et. al.*, CPV-11 poster, "J-3: Characteristics Of A Veteran Acrylic Lens Relative To Acrylic Lens Materials After Accelerated Laboratory Weathering", about 27 year veteran Phoenix M-M lenses. 11:00 Weds, 2015/4/15.

NREL
NATIONAL RENEWABLE ENERGY LABORATORY

NREL STM campus, Dennis Schroeder

مدينة الملك عبد العزيز
للعلوم و التقنية KACST

UNIVERSIDAD POLITECNICA MADRID

POLITÉCNICA
Instituto de Energía Solar

This work was supported by:

U.S. Department of Energy under Contract No. DE-AC36-08GO28308 with NREL.

The Comunidad de Madrid through the program MADRID-PV-CM (S2013/MAE2780) with IES-UPM.

Appendix (Extra Slides)

Lens Results: Measurements Comparing Lenses

- Performance of both veteran lenses reduced (vs. both reference lenses), particularly at short wavelengths. $\Delta\tau$ ~10% for APS-O-06 vs. KACST-O-06.
- Performance of palletized reference lens (KACST-R-06) worse than warehouse (NREL-W-06) reference lens at short wavelengths.

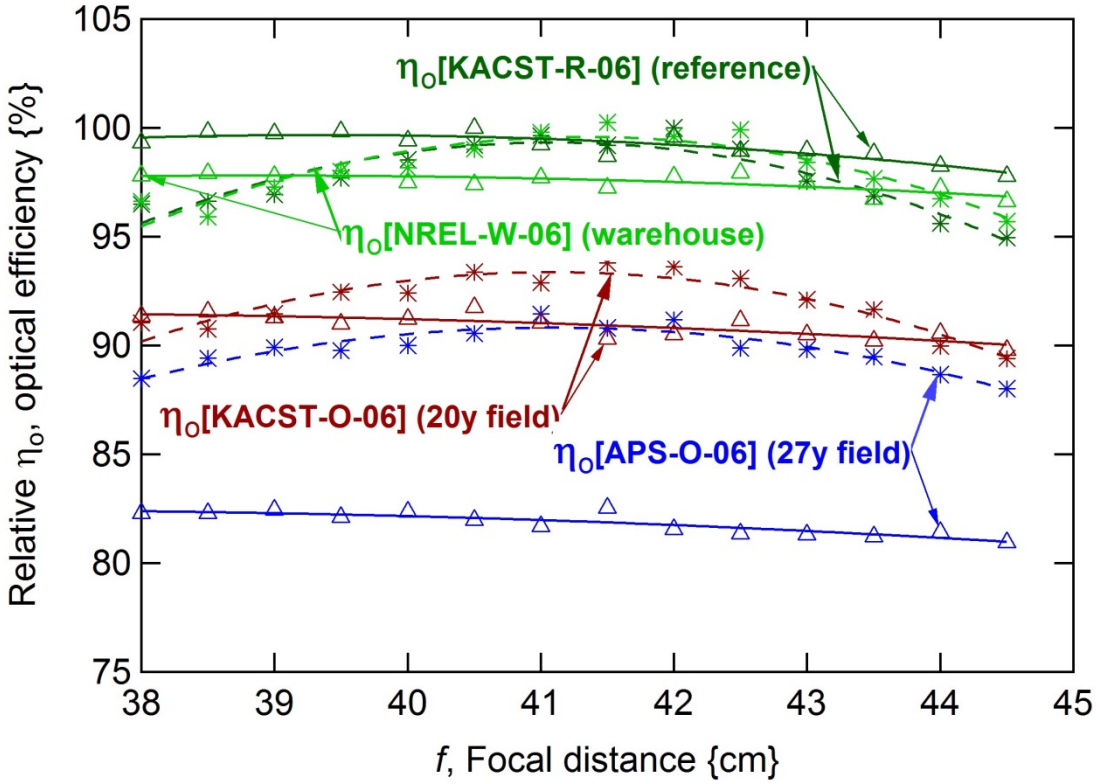

Comparison of relative ηo for the center of the lenses (± 2 S.D., 8 cm x 8 cm mask, normalized to KACST-R-06) as a function of focal distance. Scans obtained using the Si cell with the hot mirror (corresponding spectral bandwidth of 390-750 nm, indicated using a triangle with best fits using solid lines); or cold mirror (675-1150 nm, shown using asterisk and dashed lines).

Lens Results: Measurements Comparing Lenses

- η_o reduced ≥ 10% for veteran vs. reference lenses.
- $\Delta\eta_o$ greatest for APS-O-06, particularly for short wavelengths.
- $\Delta\eta_o$ greatest for KACST-O-06 on solar simulator (includes lens facets).
- $\Delta\eta_o$ (hemispherical – direct) of 7% observed for PMMA Fresnel lenses in SAND79-1791.
- $\Delta\eta_o$ greatest for NREL-R-06, particularly for short wavelengths. Some light may be lost outside of detector for flatter lens.
- Range of *f* values observed (relative to design value of 42.672 cm).

			CPV SOLAR SIMULATOR							SPECTROPHOTOMETER & ANALYSIS OF HEMISPHERICAL TRANSMITTANCE		
LENS SPECIMEN	LOCATION	CONDITION	η_o, ENTIRE LENS {%} (at 39.7 cm)	*f* , FOCAL DISTANCE {cm}	R_m, MEAN RADIUS CURVATURE {m}	$\Delta\eta_o$, ENTIRE LENS {%}	$\Delta\eta_o$, LENS CENTER {%}	$\Delta\eta_{o,HM}$ LENS CENTER {%}	$\Delta\eta_{o,CM}$ LENS CENTER {%}	$\Delta\eta_o$, (300-1150 nm) {%}	$\Delta\eta_o$, (390-750 nm) {%}	$\Delta\eta_o$, (675-1150 nm) {%}
KACST-O-06	Riyadh	field 20y	74	39.0	-0.07	-10	-8	-9	-5	-3	-3	-2
APS-O-06	Phoenix	field 27y	75	41.1	0.04	-11	-12	-18	-8	-12	-15	-10
KACST-R-06	Riyadh	reference	83	38.7	-0.08	N/A	N/A	N/A	N/A	N/A	N/A	N/A
NREL-W-06	Golden	warehouse	85	39.9	-0.01	3	-1	-2	0	-0.1	-0.6	0.3

Summary of results for lens specimens. Measurements obtained at IES-UPM were performed on lens specimens using the CPV Solar Simulator. Data was obtained for the whole lenses and then for masked lenses: with the Si cell directly (no subscript); with a hot mirror (-HM); or with a cold mirror (-CM). Measurements obtained at NREL were performed on coupon specimens cut from the lenses, with the faceted surface milled and then polished. The broadband spectral measurements are analyzed for the approximate bandwidths of the Si cell, hot mirror, and cold mirror, respectively. Efficiency values are shown in the table relative to the KACST reference specimens.

Lens Results: Measurements Comparing Lenses

$\tau_{h,lenses}$

SITE	LOCATION	CONDITION	$\Delta\eta_o$, (300-1150 nm {%}	$\Delta\eta_o$, (390-750 nm) {%}	$\Delta\eta_o$, (675-1150 nm {%}
KACST	Riyadh	field 20y	0	0	0
APS	Phoenix	field 27y	-3	-3	-2
KACST	Riyadh	reference	N/A	N/A	N/A
NREL	Golden	warehouse	-0.3	-0.3	-0.2

- Additional analysis of spectrophotometer results (previous slide)

$\tau_{h,BMP}$

SITE	LOCATION	CONDITION	$\Delta\eta_o$, (300-1150 nm {%}	$\Delta\eta_o$, (390-750 nm) {%}	$\Delta\eta_o$, (675-1150 nm {%}
KACST	Riyadh	field 20y	0	0	0
APS	Phoenix	field 27y	-3	-3	-2
KACST	Riyadh	reference	N/A	N/A	N/A
NREL	Golden	warehouse	0.2	0.2	0.2

$\tau_{d,BMP}$

SITE	LOCATION	CONDITION	$\Delta\eta_o$, (300-1150 nm {%}	$\Delta\eta_o$, (390-750 nm) {%}	$\Delta\eta_o$, (675-1150 nm {%}
KACST	Riyadh	field 20y	-3	-3	-2
APS	Phoenix	field 27y	-12	-15	-10
KACST	Riyadh	reference	N/A	N/A	N/A
NREL	Golden	warehouse	-0.1	-0.6	0.3

$\tau_{h,BMP,\ FP}$

SITE	LOCATION	CONDITION	$\Delta\eta_o$, (300-1150 nm {%}	$\Delta\eta_o$, (390-750 nm) {%}	$\Delta\eta_o$, (675-1150 nm {%}
KACST	Riyadh	field 20y	0	0	0
APS	Phoenix	field 27y	-2	-3	-2
KACST	Riyadh	reference	N/A	N/A	N/A
NREL	Golden	warehouse	0.7	0.7	0.7

$\tau_{d,BMP,\ FP}$

SITE	LOCATION	CONDITION	$\Delta\eta_o$, (300-1150 nm {%}	$\Delta\eta_o$, (390-750 nm) {%}	$\Delta\eta_o$, (675-1150 nm {%}
KACST	Riyadh	field 20y	1	2	1
APS	Phoenix	field 27y	-7	-9	-5
KACST	Riyadh	reference	N/A	N/A	N/A
NREL	Golden	warehouse	0.6	0.7	0.4

Summary of results for lens specimens. Measurements obtained at IES-UPM were performed on lens specimens using the CPV Solar Simulator. Data was obtained for the whole lenses and then for masked lenses, obtained for the Si cell directly, with a hot mirror, or with a cold mirror. Measurements obtained at NREL were performed on coupon specimens cut from the lenses, with the faceted surface milled and then polished. For the broadband spectral measurements are analyzed for the approximate bandwidths of the Si cell, hot mirror, and cold mirror, respectively. Efficiency values are shown in the table relative to the KACST reference specimens.

Lens Results: Spectral Measurements Using MJ Cell

Optical efficiency for KACST-R-06 (reference): top junction (blue), middle junction (red)

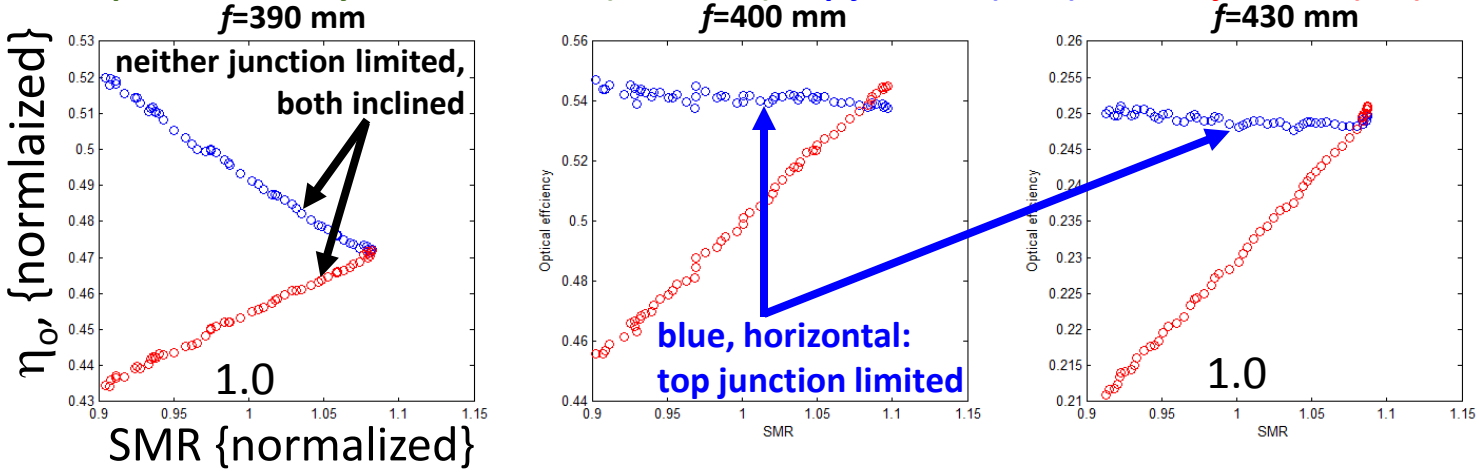

Optical efficiency for KACST-O-06 (field): top junction (blue), middle junction (red)

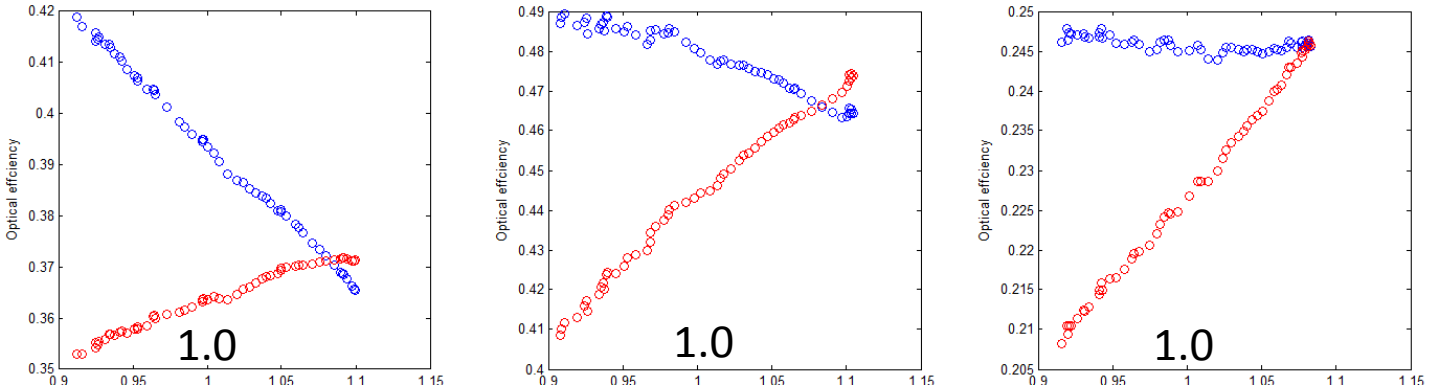

- Could contemporary CPV junctions be affected by the aged lenses?
- Focused spot falls outside MJ cell (even at optimum focal distance), reducing η_o here.
- Characterizations identify multijunction system can be current limited in red-rich light (dawn & twilight), but does not become middle junction limited.
- KACST field/reference: I_{sc} loss (at SMR=1) for MJ cell of 12.5% at f = 400 mm.
- Similarly, I_{sc} loss of 6% for Si cell.
- Reference lens not perfectly flat or degradation free.

Quantifying Direction and Magnitude of Lens Curvature

- Method: Measure the Fresnel reflections (a checkerboard pattern) at the lens first surface.
- Local curvature is calculated from the deformation of the checkered pattern squares.
- Both concave and convex shapes observed!

Reference (method): Herrero et. al., Opt. Express 23, A1030-A1039 (2015).

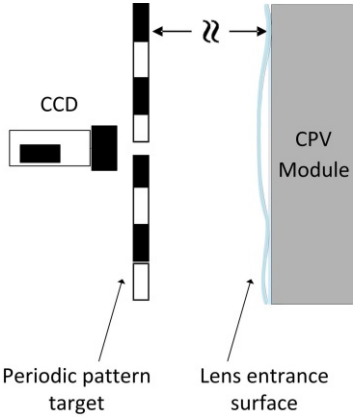

Schematic of the configuration, optical images, and results for the checkerboard test.

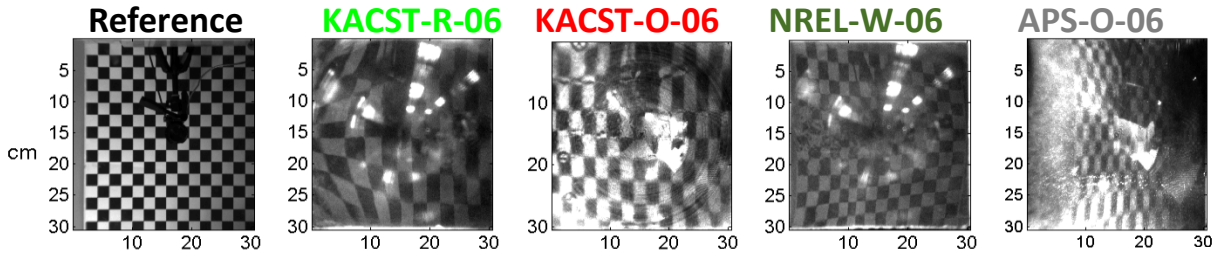

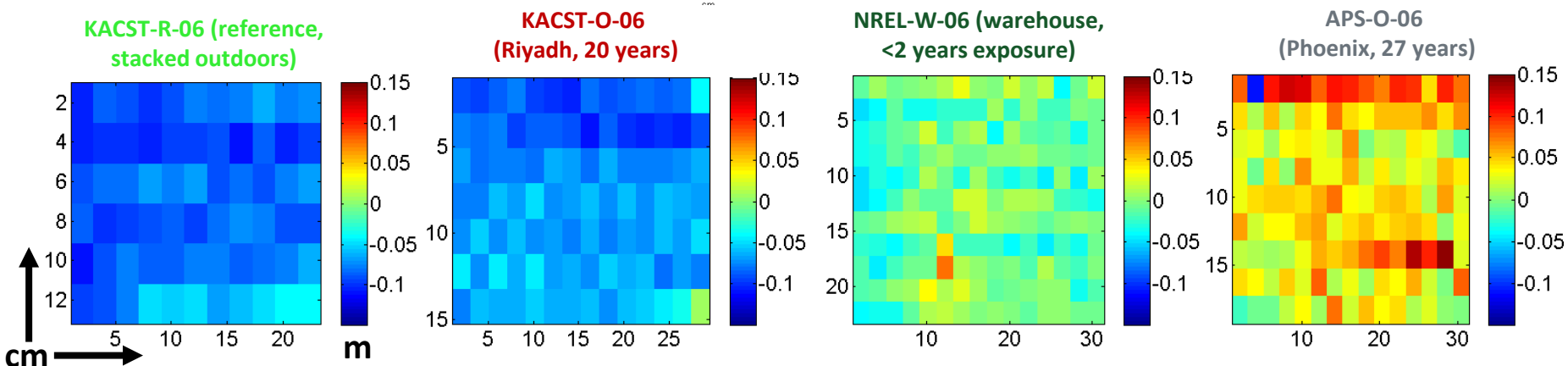

Lenses performance must be compared with same subcell limitation…
How can we assume some subcell limitation?

-The solar simulator provides a light pulse that varies with time (different spectral conditions → different SMR values)

-The limitation diagram is used to evaluate the current limitation of each subcell in the multi-junction solar cell during a single light pulse

- Horizontal trend in normalized current → subcell limitation

$$\frac{I_{MJ}}{DNI_{subcell\ (top\ or\ middle)}}$$

Instead of normalized current, the optical efficiency can be plotted

Local current top/middle mismatch due to chromatic aberration

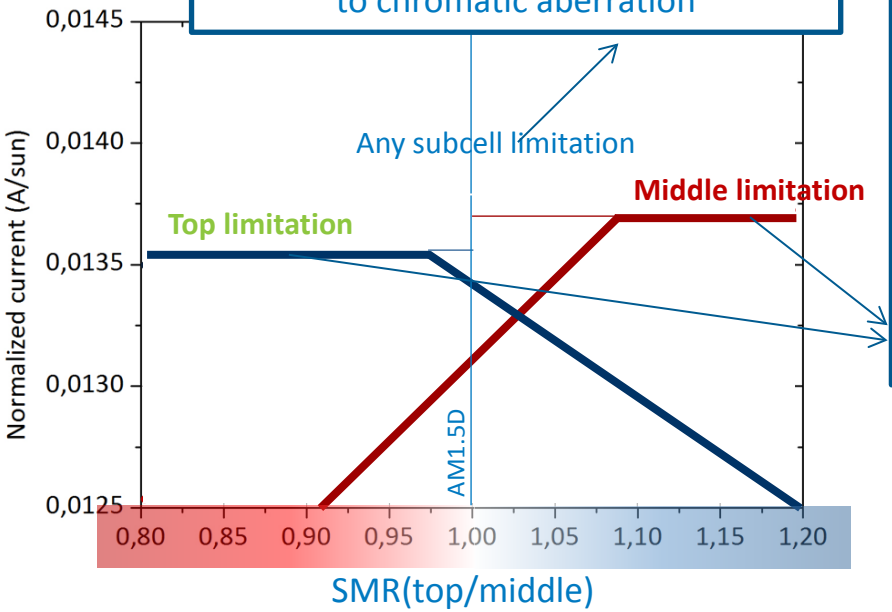

Different SMR values within the light pulse

These two values are related to the current generated by the device under test when the cell is limited by top or middle subcells

The higher the value the better the lens performance

Optical efficiency measurements at the solar simulator (for Si cell)

-Lenses are measured at constant irradiance at different focal distances:

- Includes low pass (hot mirror, "HM") and high pass (cold mirror, "CM")

RAN (Riyadh reference)
RAO (Riyadh fielded 20 years)
PAM (Phoenix- Martin-Marietta)
NUW (NREL warehouse)

Example of Si cell SR and SR filtered by CM and HM

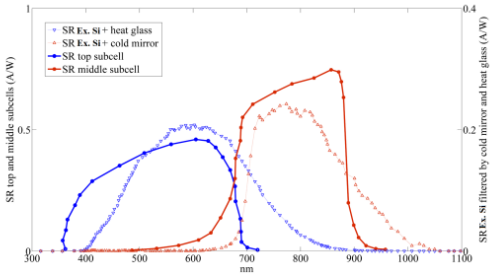

Top wavelengths

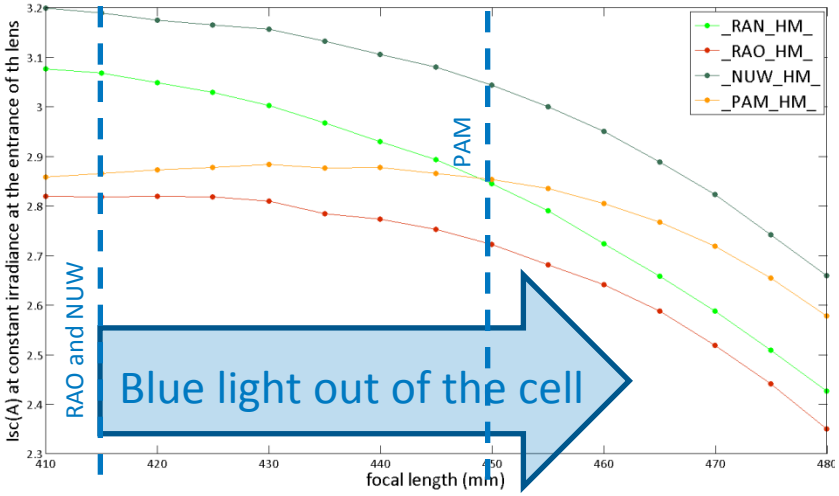

Middle wavelengths

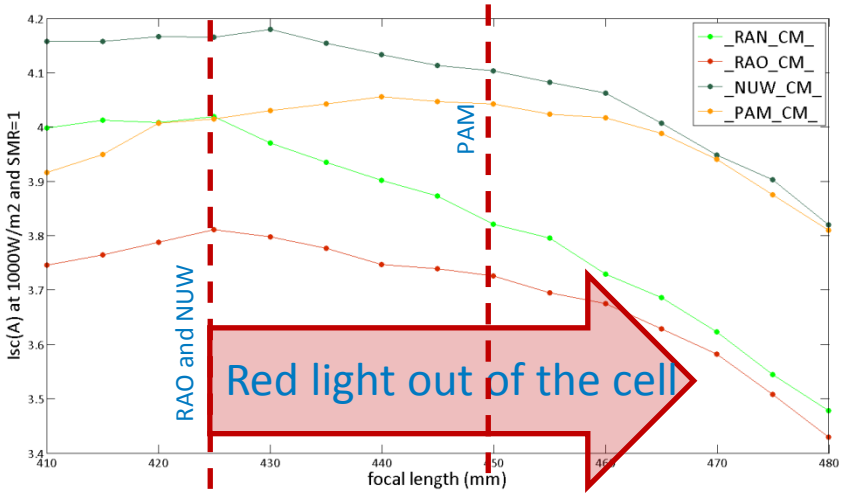

- The convex lens (PAM) has a larger optimum focal distance than the others… therefore, both blue and red light falls outside the cell (current starts to decrease) at larger focal lengths if compared with the other lenses.
- The more concave lens (RAN) decreases performance faster at larger focal distances.
- The flat lens (NUW) and the less concave shape (RAO) have similar performance.
- Due to neutral filters (to avoid loss of linearity of Si cell) and CM/HM filters (to discriminate between wavelengths) the absolute value of effective irradiance is unknown but it is assumed to be constant.

Haze: Riyadh vs. Phoenix vs. References

- Portions of lens measured: (1) as-received, "lens"; (2) after milling and polishing back surface, "bmp"; and (3) after polishing front (field) surface, "bmp,fp".
- Values: Riyadh 20y field (approaching 3% at 400 nm); Phoenix 27y field (→ 11% at 400 nm); Phoenix 22y (→ 8% at 400 nm) Riyadh reference approaching (→ 12% at 400 nm); Golden warehouse (→ 9% at 400 nm).
- ~1% difference in τ_h with and without facets present. •Rounded cut-on transition from optical scattering (not discoloration) •Increased haze for front polished references
- Polishing clearly helped partially restore transmittance for most lenses, except Phoenix 27y. This suggests that a significant portion of the haze comes from damage at the material surface. (h<100 μm). The Phoenix 27y sample is damaged deep into the material, which could see observed visually on a sample polished on its edge (damage is ≥0.5mm depth).
- The Phoenix 20y sample clearly has the worst transmittance characteristics.
- The NREL warehouse sample had some surface damage from cleaning (evident in scratches observed in SEM, AFM).

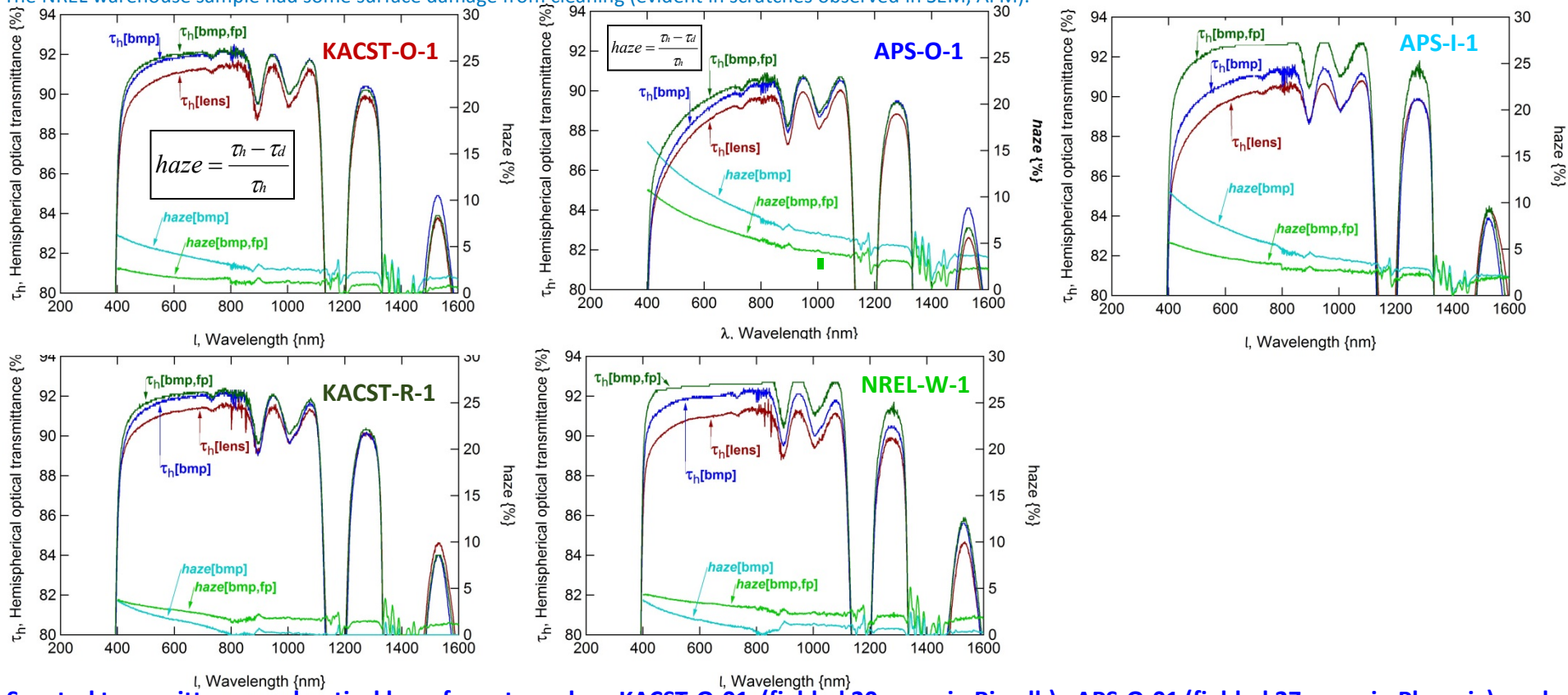

Spectral transmittance and optical haze for veteran lens KACST-O-01 (fielded 20 years in Riyadh) , APS-O-01 (fielded 27 years in Phoenix), and APS-I-01 (fielded 22 years in Phoenix) as well as reference lenses KACST-R-01 (stored outside in stack) and NREL-W-01 (stored in a warehouse after brief field use). The transmittance of the original lens ("lens") is shown relative to the same lens with the back milled and polished ("bmp"), and then subsequently polished on the front ("bp,fp"). Measurements for the polished samples have been compensated to the nominal lens thickness of 4.51 mm. The haze is determined as the percent difference in the hemispherical and direct transmittance.

Summary of Optical Performance (Lenses Processed at NREL)

- UV cut-off of ~273 changed by ≤ 6 nm between test & reference
- Maximum *YI* of 3.3 observed for specimens.
- All specimens had neutral colorcast. *YI* may follow from rounded cut-on transition, not discoloration.

LENS TRANSMITTANCE, AS-RECEIVED, AFTER CLEANING								
LOCATION	CONDITION	τ_{sw} (280-2500 nm) {%}	τ_{rsw} (300-1250 nm) {%}	τ_{swJ1} (300-650 nm) {%}	τ_{swJ2} (650-890 nm) {%}	τ_{swJ3} (890-1800 nm) {%}	λ_{cUV} {nm}	*YI* {unitless}
Riyadh	reference	77.0	88.4	86.8	91.2	76.9	373	1.3
Golden	warehouse	76.7	88.0	86.4	91.0	76.4	376	1.2
Riyadh	field 20y	76.3	88.0	86.4	91.1	75.8	375	1.6
Phoenix	field 27y	74.6	85.8	82.9	89.2	74.8	379	3.3
Phoenix	field 22y	77.0	87.5	85.1	90.2	77.9	372	2.4
DIFFERENCE[FACETED SURFACE MILLED AND POLISHED, ORIGINAL LENS]								
LOCATION	CONDITION	τ_{sw} (280-2500 nm) {%}	τ_{rsw} (300-1250 nm) {%}	τ_{swJ1} (300-650 nm) {%}	τ_{swJ2} (650-890 nm) {%}	τ_{swJ3} (890-1800 nm) {%}	λ_{cUV} {nm}	*YI* {unitless}
Riyadh	reference	-0.6	0.2	0.5	0.6	-1.4	2	0.1
Golden	warehouse	0.5	0.8	1.0	0.9	0.2	1	-0.3
Riyadh	field 20y	0.8	0.7	0.8	0.7	0.9	-1	-0.1
Phoenix	field 27y	0.7	0.6	0.5	0.7	0.8	0	0.1
Phoenix	field 22y	-0.9	0.2	0.7	0.7	-2.2	3	-0.3
DIFFERENCE[INCIDENT SURFACE MILLED AND POLISHED, FACETED SURFACE MILLED AND POLISHED]								
LOCATION	CONDITION	τ_{sw} (280-2500 nm) {%}	τ_{rsw} (300-1250 nm) {%}	τ_{swJ1} (300-650 nm) {%}	τ_{swJ2} (650-890 nm) {%}	τ_{swJ3} (890-1800 nm) {%}	λ_{cUV} {nm}	*YI* {unitless}
Riyadh	reference	-1.4	-2.2	-3.1	-2.2	-0.6	-1	0.6
Golden	warehouse	-1.6	-2.0	-2.7	-2.1	-1.1	0	0.7
Riyadh	field 20y	-1.2	-1.3	-1.6	-1.3	-1.1	0	0.5
Phoenix	field 27y	-4.7	-5.8	-7.7	-5.9	-3.2	0	2.3
Phoenix	field 22y	-2.3	-2.9	-4.0	-2.9	-1.4	0	1.2

Summary of performance, including hemispherical transmittance (with the corresponding wavelength range identified); λ_{cUV}; and *YI* for the lens samples. The difference in performance is shown for successive refinement (polishing) of the lenses in the tables (values calculated for processed minus the previous state).

Reflectance: Riyadh vs. Phoenix vs. References

- Measurable reflectance obtained down to ~390 nm for unpolished lens specimens. Reflectance looks to be limited by roughness of the material (rolls down at 390 nm); refractive index is not a useful explanation (does not increase below 390 nm).
- Reference samples show the highest ρ, consistent with expectation that veteran lenses would be roughened at their first surface by field weathering.
- Measurements for NREL warehouse (open integrating sphere) are substantially lower (less reflective) than the other materials, so ρ_{direct} is greater for those specimens. Consistent for 3/3 specimens. Enabling factor: unknown.

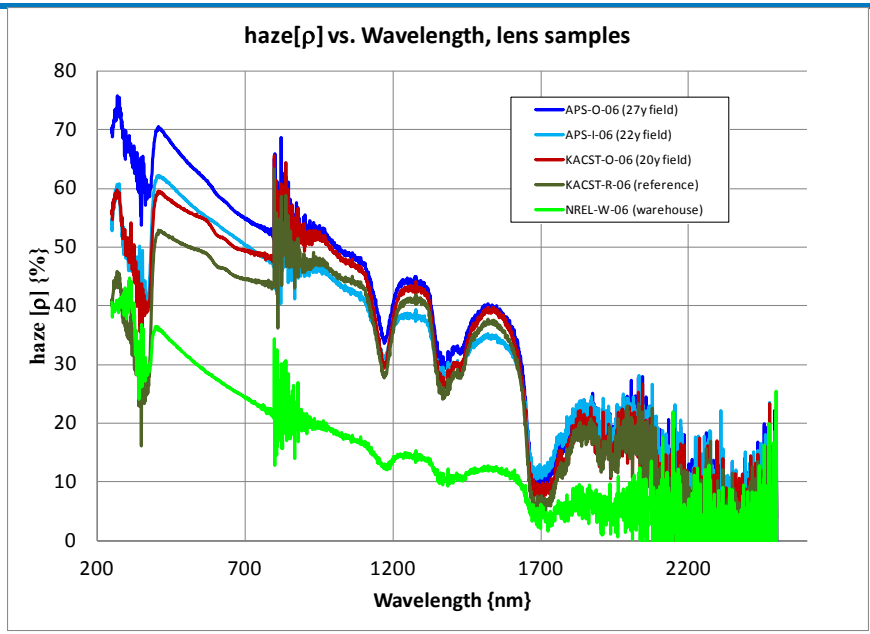

Direct reflectance for lens specimens as received from the field or other conditions.

- Measurable reflectance down to ~390 nm for polished specimens is consistent with expected trend for refractive index, *n*, which should increase approaching the fundamental band edge. Increased *n* is observed for the polished specimens until *n* is limited by the additives.

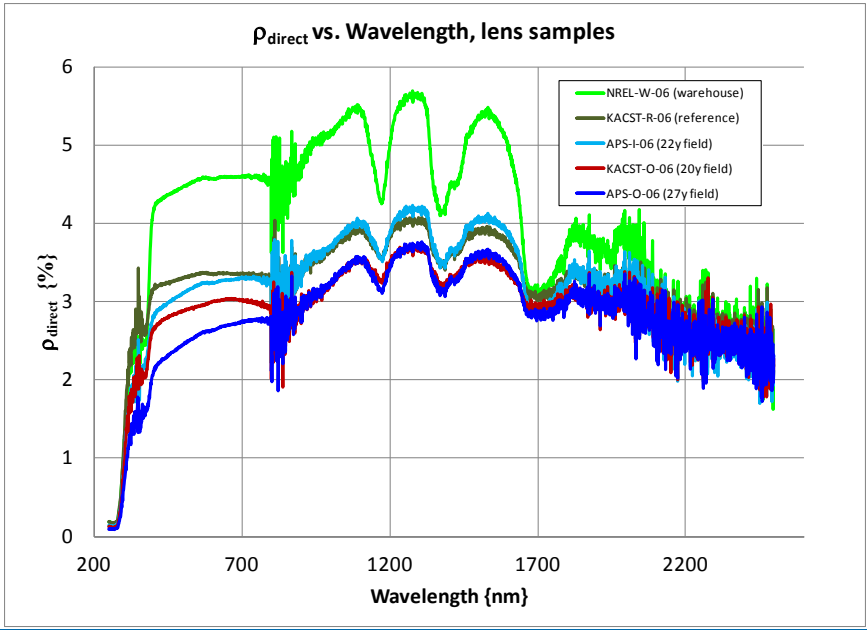

Direct reflectance for lens specimens after milling the facets and polishing the back and front surfaces.

Haze[Reflectance]: Riyadh vs. Phoenix vs. References

- Phoenix 27y field specimen has haze well into the thickness of the lens (only sample with increasing haze below 800 nm after polishing). Not enough of the surface was removed to restore its ρ like the other specimens. A haze on the order of ~1 mm could be observed as the side of the polished Evonik samples (Miller et. al., "Characteristics of a Veteran Acrylic Lens Relative to Acrylic Lens Materials After Accelerated Laboratory Weathering", Proc. Intl. CPV Conf., 2015).

Haze[reflectance] for lens specimens as received from the field or other conditions.

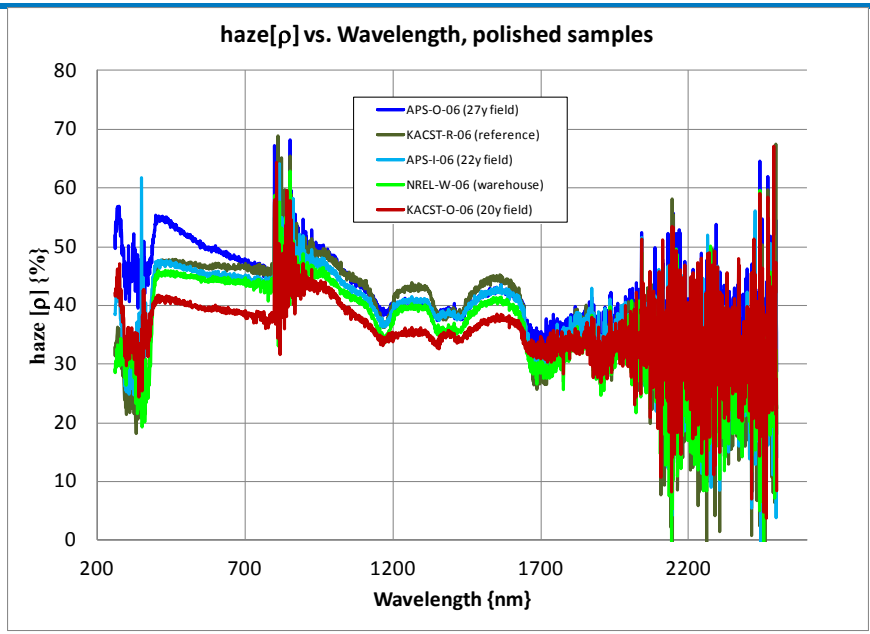

Haze[reflectance] for lens specimens after milling the facets and polishing the back and front surfaces.

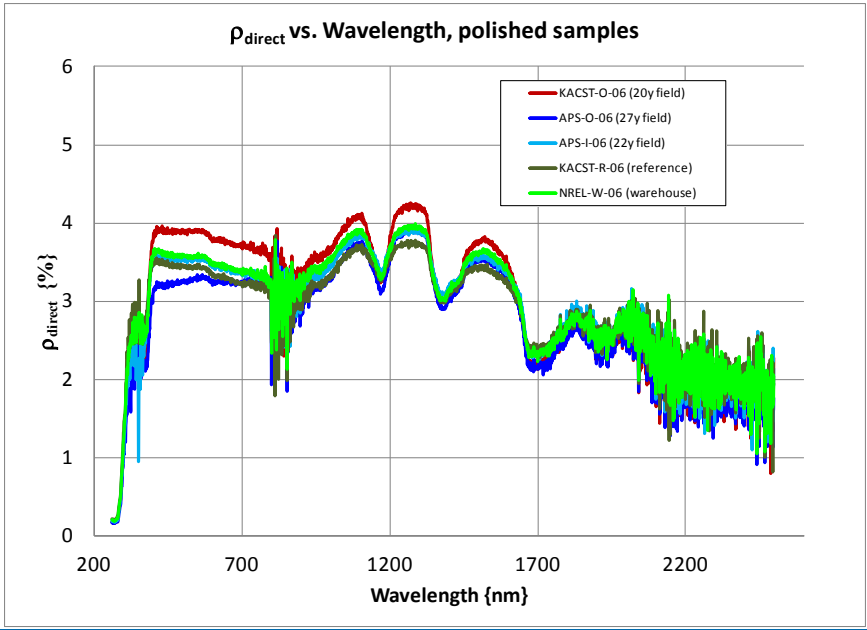

Characterization of Optical Scattering

- τ_d is reduced (on the order of ~3%) as the acceptance angle is reduced.
- τ_d most affected for Martin-Marietta and Intersol veteran lenses.
- Literature: $\Delta\tau_d$ of ~1% with θ_a (from 1 to 15 mrad). Inflection at θ_a ~2 mrad. (comparable to reference and KACST-O-07 coupons).
- Offset between stock specimen & reference coupons may follow from curvature & lack of parallelness for the manually polished coupons.
- Rank order for VLABS instrument consistent with spectrophotometer characterization.
- τ_d of 90.7 for KACST-R-01 suggests spectrophotometer θ_a is on order of 2-3°.

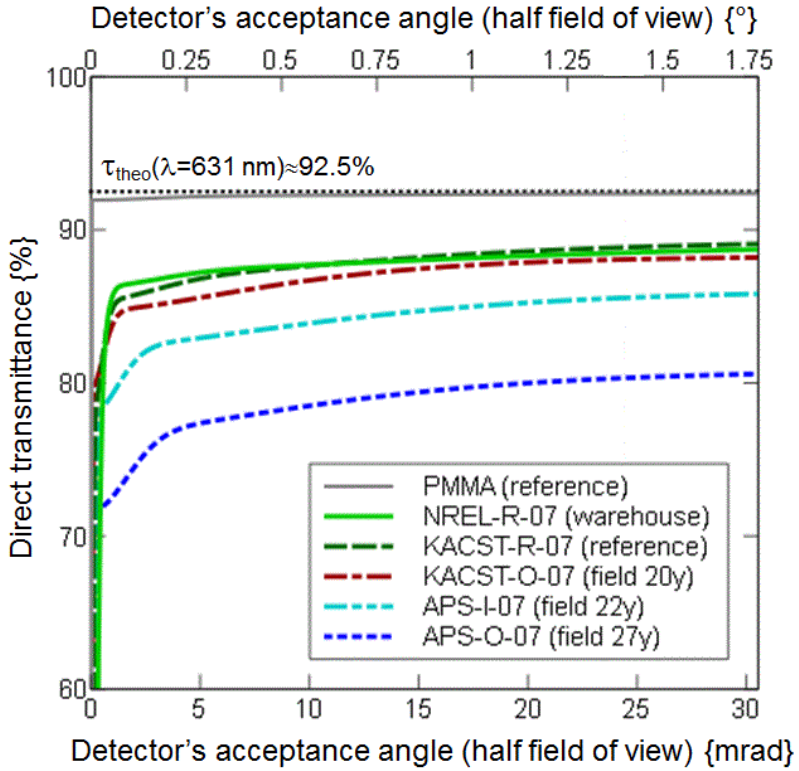

- 0.2-0.3% reduction in τ_d predicted for changing specimen thickness from 2.17mm (stock PMMA reference) to 4.5 mm (M-M-lens).
- Lesser τ_d at right of figure likely follows from processes of optical absorption, backscattering, and wide-angle forward scattering as well as the ambient humidity.

Optical scattering as a function of incident angle (half field of view) for coupon specimens with the faceted surface milled and polished. The theoretical maximum transmittance for PMMA is indicated in the figure relative to a measure stock sheet specimen.

Comparing The Surface Integrity of the Lenses

- Voids on order of 10's of μm's on first surface of APS M-M only. Porosity extends ≥1 mm into surface.

True location of epoxy/specimen interface may actually occur higher in figure.

- Other samples (including APS Intersol) not overtly affected other than local surface roughness (waviness) at high magnification.
- No evidence of crazing or cracking into the surface of the specimen was observed in the AFM and SEM characterizations.
- APS-O-08: porosity easily explain $\Delta\eta o$, with inability to restore by polishing the front surface.
- Pores may follow from solvent/ESC damage. Maybe during lens production (pressure too low).

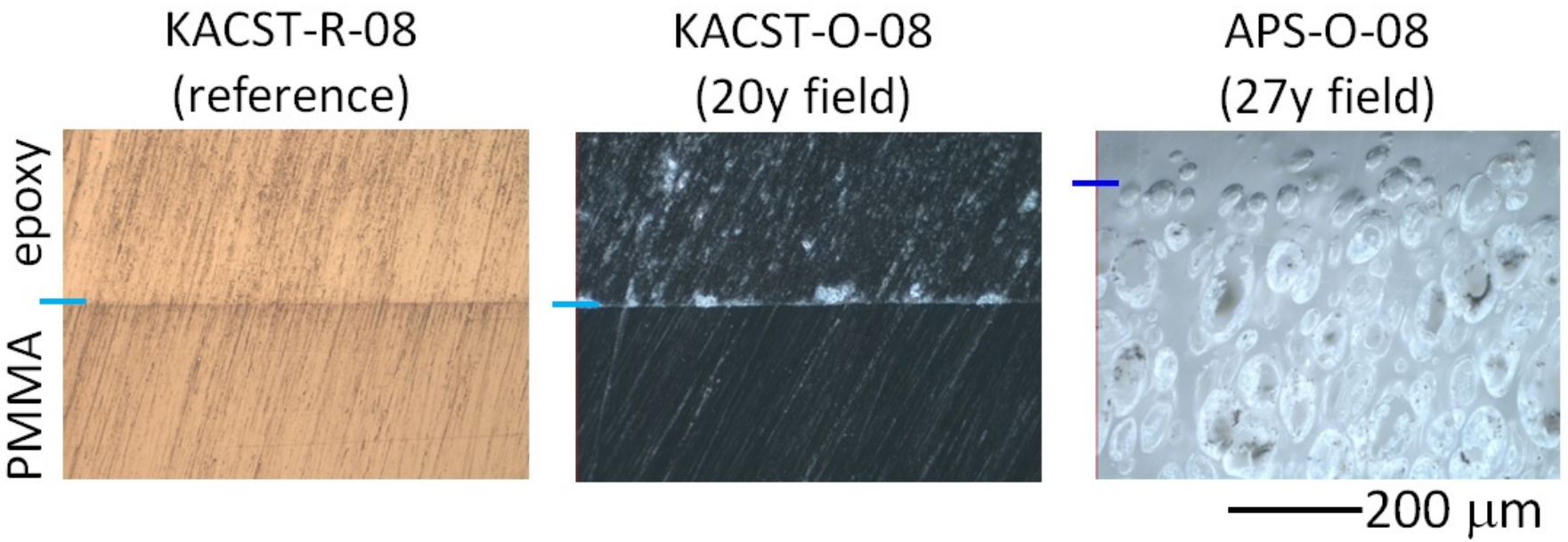

Comparison of the surface integrity of the lens specimens. Representative optical miscopy images are shown for the KACST lenses (reference and fielded 20y) as well as an APS lens (fielded 27y). The location of the interface between the potting epoxy and the PMMA lens is indicated with a hash mark at the left of each image.

Comparing The Facet Geometry of the Lenses

- Within the margin of error, valley radius similar between all lenses examined.
- Tip radius was certainly less for APS Intersol lens, possibly also APS M-M lens.
- Intended prism radius for lens was 2.54 μm. (Larger actual size reduces η_o).
- Limited # of measurements (6) here, but same diamond typically used for mold cutting across the lens.
- Disparate radii for APS suggests different vendors (consistent with their shared fluorescence spectra).
- Similar radii between test & reference specimens (KACST relative to KACST & NREL) implies prism geometry should not motivate disparate performance (haze).

SITE	SITE LOCATION	SPECIMEN DESIGN	SPECIMEN HISTORY	R_t {μm}	R_v {μm}
NREL	Golden	M-M	warehouse	29±1	7±1
KACST	Riyadh	M-M	reference	35±11	4±3
KACST	Riyadh	M-M	field 20 y	20±7	3±1
APS	Phoenix	M-M	field 27 y	15±2	8±3
APS	Phoenix	Intersol	field 22 y	6±5	4±1

Summary of the prism tip (Rt) and valley (Rv) radius for the various lens specimens. Estimates were obtained from scanning electron and optical images of sectioned coupon specimens.).

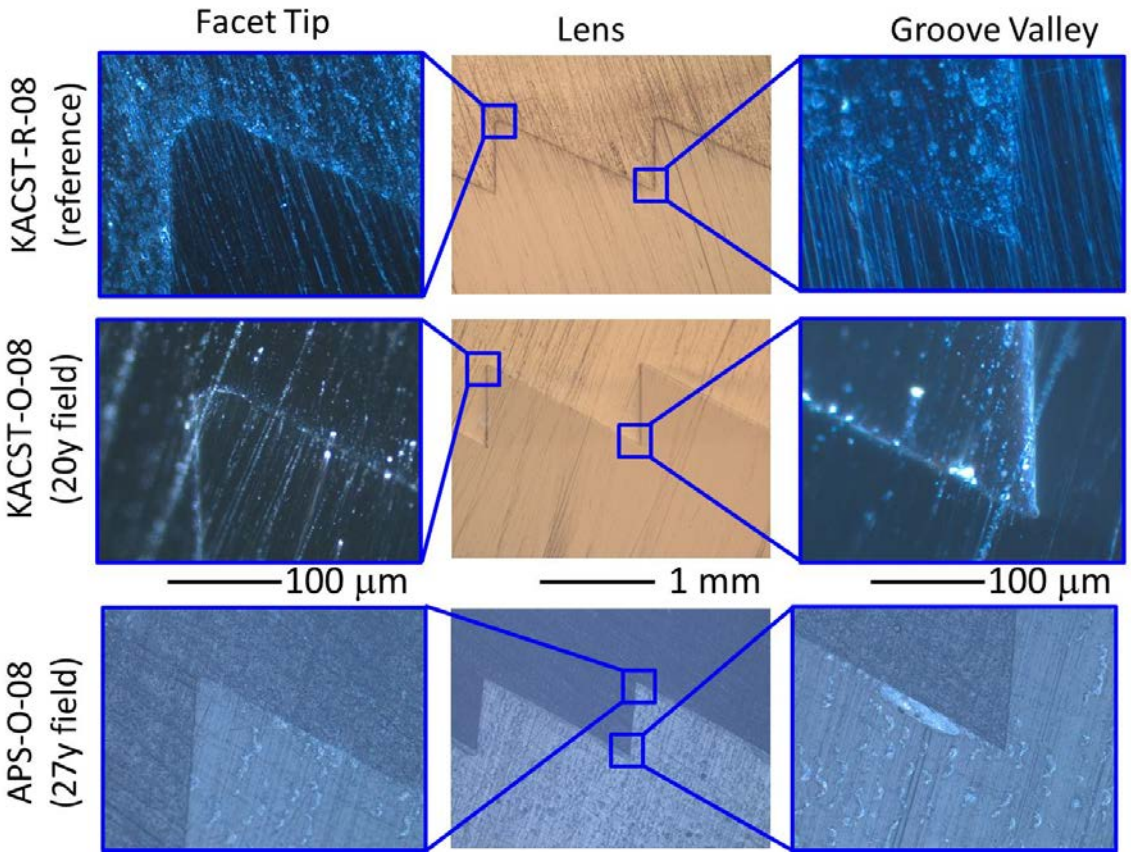

Comparison of the lens facet geometry for the reference and field KACST specimens. Representative optical miscopy images are shown for: the faceted surface of the lens (center, at lesser magnification); the facet tip (left, at higher magnification); and the facet valley (right, at higher magnification).

M_w Data

- Back surface M_p & M_w measurements (*e.g.*, used for reference values) not highly consistent, but typically exceed 80,000 g·mol^{-1}. Bulk M_w approaches 110,000 g·mol^{-1} in Miller et. al., Proc Intl. Conf. CPV, 2015.
- The average difference between front and back (field or module-interior facing) is comparable to the effect of field aging, *e.g.*, KACST 20 y vs. KACST reference.
- Negligible difference in breadth of the M_i distribution profile (*PD*), *i.e.*, no change in distribution profile - just reduction in average M_i on front side.
- No strong chain scission here. More severe results from accelerated artificial aging (via random chain scission from UV) in: Miller et. al., SOLMAT, 111, 2013, 165-180. Extreme results (formation of through thickness cracked network and spalling of first surface) for APS M-M specimens (molecular weight on order of 10,000) subject to same aging regiment.

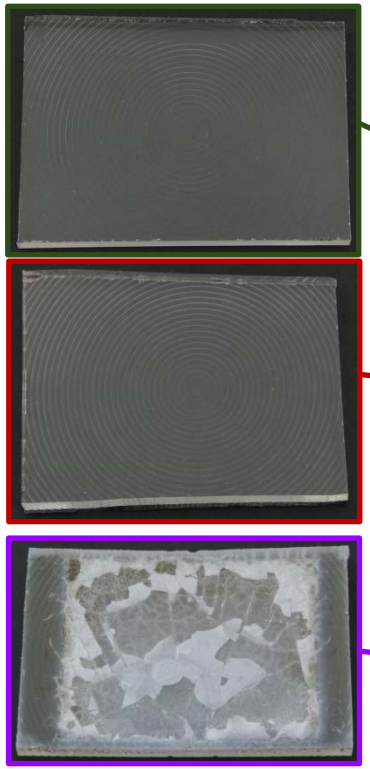

SITE	SITE LOCATION	MODULE MAKE	SPECIMEN HISTORY	LENS SURFACE	M_p {g·mol^{-1}}	M_n {g·mol^{-1}}	M_w {g·mol^{-1}}	*PD* {unitless}
NREL	Golden	M-M	warehouse	incident	81,000	32,000	90,000	2.77
NREL	Golden	M-M	warehouse	faceted	109,000	34,000	102,000	2.99
KACST	Riyadh	M-M	reference	incident	51,000	23,000	59,000	2.64
KACST	Riyadh	M-M	reference	faceted	84,000	31,000	91,000	2.97
KACST	Riyadh	M-M	field 20 y	incident	52,000	24,000	60,000	2.54
KACST	Riyadh	M-M	field 20 y	faceted	73,000	29,000	85,000	2.97
APS	Phoenix	M-M	field 27 y	incident	48,000	20,000	57,000	2.95
APS	Phoenix	M-M	field 27 y	faceted	73,000	31,000	84,000	2.72
APS	Phoenix	Intersol	field 22 y	incident	47,000	22,000	56,000	2.50
APS	Phoenix	Intersol	field 22 y	faceted	65,000	31,000	76,000	2.44
all	all	all	all	(faceted-incident)	25,000	7,000	23,000	0.14
NREL	indoor	M-M (from APS)	Ci4000 aged 3 y	incident	7,000	3,000	10,000	3.09
APS-NREL	APS-NREL	M-M (from APS)	field 27 y-aged 3 y	($APS_{faceted}$-$Ci4000_{incident}$)	66,000	28,000	74,000	-0.37

Molecular weight data for the lens specimens, including: the peak (M_p); number average (M_n); and weight-average (M_w) weights, as well as the polydispersity (*PD*). The module design is distinguished between the manufacturers: Martin-Marietta (M-M) or Intersol.

For details regarding the weathering (3y cumulative Xe at 60C/60%) of sample (f), see Ref. Miller et. al., SOLMAT, 111, 2013, 165-180.

UV-VIS Fluorescence Spectroscopy

- The different spectra for the APS samples suggests a different material formulation was used. ≥2 PMMA formulations and/or vendors. , e.g., injection molded
- The lack of signal for indoor specimen suggests the loss of additive(s).
- The similar intensity for the KACST reference and field specimens suggests the responsible formulation additives remain intact.
- The spectra for the KACST reference and field specimens are different from those previous examined; spectra for the APS samples share peaks with of a haze prone specimen. **Miller et. al, SOLMAT, 111, 2013, 165-180. (DOI: dx.doi.org/10.1016/j.solmat.2012.05.043)**

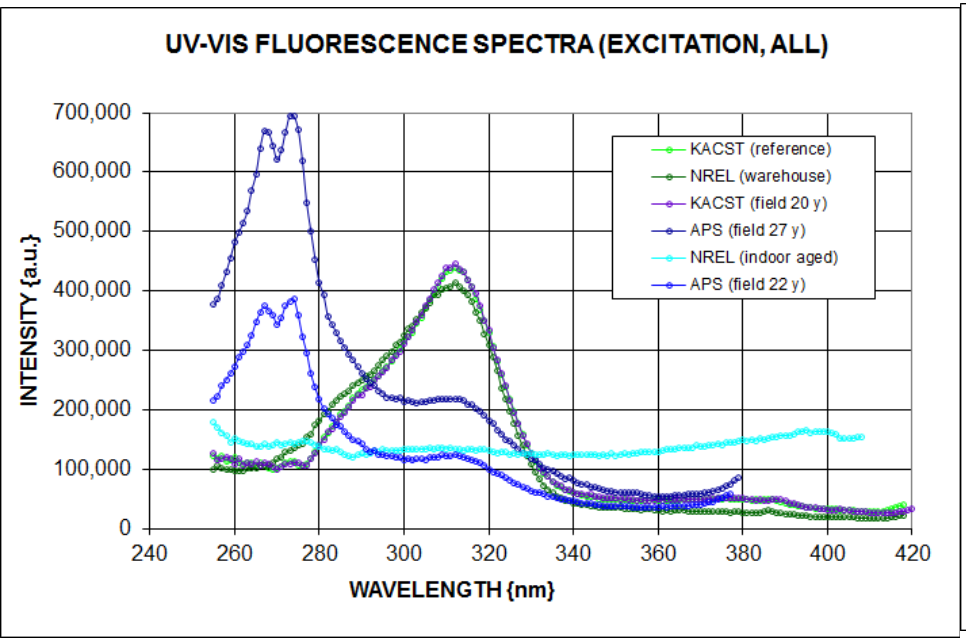

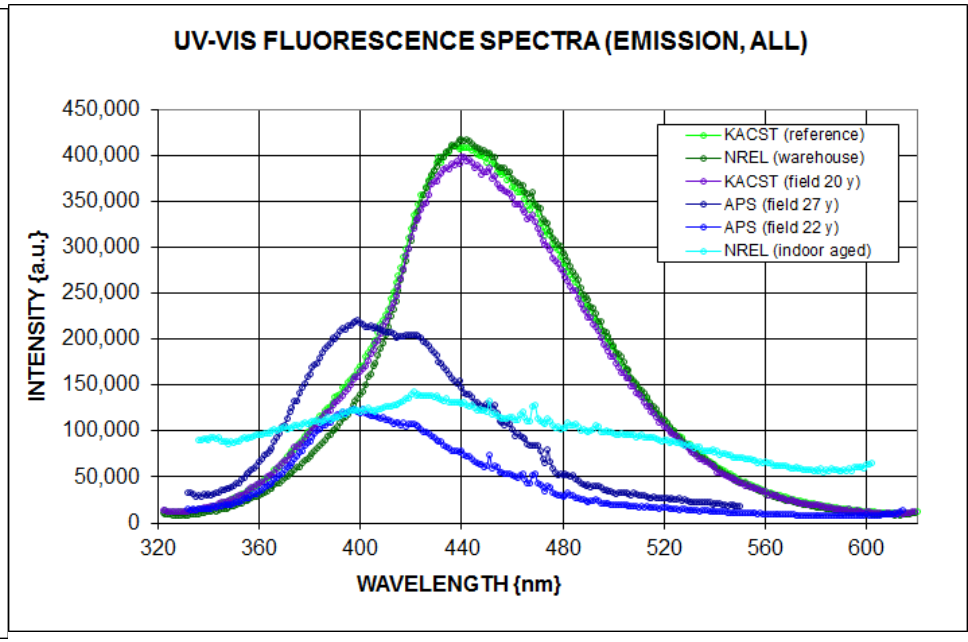

Excitation and emission peak pairs for the samples investigated. The most significant emission peaks and their corresponding excitation spectra are shown. The indoor specimen was aged in a Ci4000 Weather-ometer at 2.5x the AM1.5 UV spectrum at 60 °C and 60% RH for 36 months.

Gas Chromatography-Mass Spectroscopy

- NREL solvent: 75 wt% dichloromethane; 12.5 wt% petroleum ether; 12.5 wt% methanol.
- Results consistent with the lenses from APS (M-M and Intersol modules) both being a different formulation from that used in Riyadh (as suggested in fluorescence spectroscopy).
- Some additives may not be detected or identified in GC-MS. For example a UV Absorber is implied from the λ_{cUV} in the transmittance spectra of the PMMA's. A UV Stabilizer may also be present in the NREL warehouse sample (as present in the Phoenix sample).

NREL Lens (NREL-W-X, warehouse)				
Compound Name	Primary R.T. {s}	Secondary R.T. {s}	Peak Area {mV·s}	Likely Use
2-Propenoic acid, ethyl ester	90	1.24	107,081	comonomer
2-Propenoic acid, 2-methyl-, methyl ester	90	1.28	3,981,530	unreacted monomer (or pyrolysis product of)
1-Hexene, 5-methyl-	326	1.01	61,534	impact modifier (olefin)
1-Octene	442	1.06	208,082	impact modifier (olefin)
3-Tetradecene, (Z)-	638	1.13	66,031	impact modifier (olefin)
1,2-Cyclohexyldicarboxylic acid, diester	730	1.62	137,618	dimer of starting monomer
n-Tetradecanol	838	1.41	628,032	processing aid (alcohol)
1-Octadecene	854	1.38	86,504	impact modifier (olefin)
n-Octadecanol	858	1.23	196,664	processing aid (alcohol)
1-Hexaadecanol, acetate	878	1.38	161,259	processing aid (alcohol)

Phoenix Lens (APS-O-X, 27 years in field)				
Compound Name	Primary R.T. {s}	Secondary R.T. {s}	Peak Area {mV·s}	Likely Use
2-Propenoic acid, ethyl ester	86	1.23	368,403	comonomer
2-Propenoic acid, 2-methyl-, methyl ester	90	1.28	7,145,877	unreacted monomer (or pyrolysis product of)
Tetramethylbutanedinitrile	330	2.22	1,400,842	residual initiator
Methyl salicylate	450	1.43	735,175	UV stabilizer
1,2-Cyclohexyldicarboxylic acid, diester	730	1.63	151,130	dimer of starting monomer
Dodecanoic acid, methyl ester	778	1.32	266,669	plasticizer (fatty acid)
Dodecanoic acid, ethyl ester	802	1.33	206,965	plasticizer (fatty acid)
Tetradecanoic acid, methyl ester	822	1.28	390,940	plasticizer (fatty acid)
Tetradecanoic acid, ethyl ester	850	1.35	188,740	plasticizer (fatty acid)
Hexadecanoic acid, methyl ester	874	1.35	161,713	plasticizer (fatty acid)
Hexadecanoic acid, ethyl ester	890	1.34	350,355	plasticizer (fatty acid)

Major peaks in lens samples, from match of peak spectra to NIST library spectra. Samples from a lens stored in a warehouse at NREL (believed to be the same material used in Riyadh) and a lens deployed for 27 years in Phoenix were examined. There was no injection of known compounds to confirm identification by retention time and spectra. The composition, retention time (R.T., for the primary and secondary retention), and area of the peak examined are given in the table. The likely use is also speculated in the tables for the contents identified.

AFM and SEM: Roughness Minor Contribution to the Haze

- Specimens measured after DI H_20 rinse (to remove contamination).
- Series of scans performed.

(90 x 90 and 20 x 20 μm in AFM; 2 x 2 mm → 20 x 20 μm in SEM).

- Sizeable (μm's x mm's) surface scratches observed in some scans. (may result from handling).
- Smaller (~10's nm) localized roughness observed in areas.
- Could include residual surface: contamination and porosity.

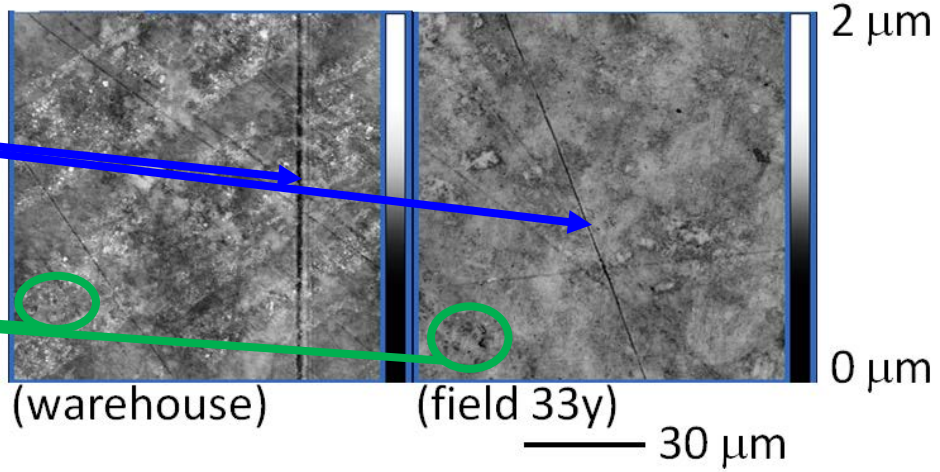

Corresponding representative micrographs and tabulated AFM scans of veteran and reference lenses. The average (R_a), root-mean-square (R_{rms}), and peak-to-valley (R_{PV}) roughness are reported for the 90 μm x 90 μm scans. (averaged from 3 separate measurements)

SPECIMEN	CONDITION	R_a {nm}	R_{rms} {nm}	R_{pv} {nm}
KACST-W-06	reference	48	62	873
KACST-O-06	field 20 y	84	115	1,225

- Same order of magnitude roughness observed in all specimens. → λ/4.
- Roughness values provided here for subsequent optical analysis of τ.
- Tip and surface contamination may affect measurements.
- Another mode, *i.e.*, crazing, may more significantly contribute to haze.

AFM Data

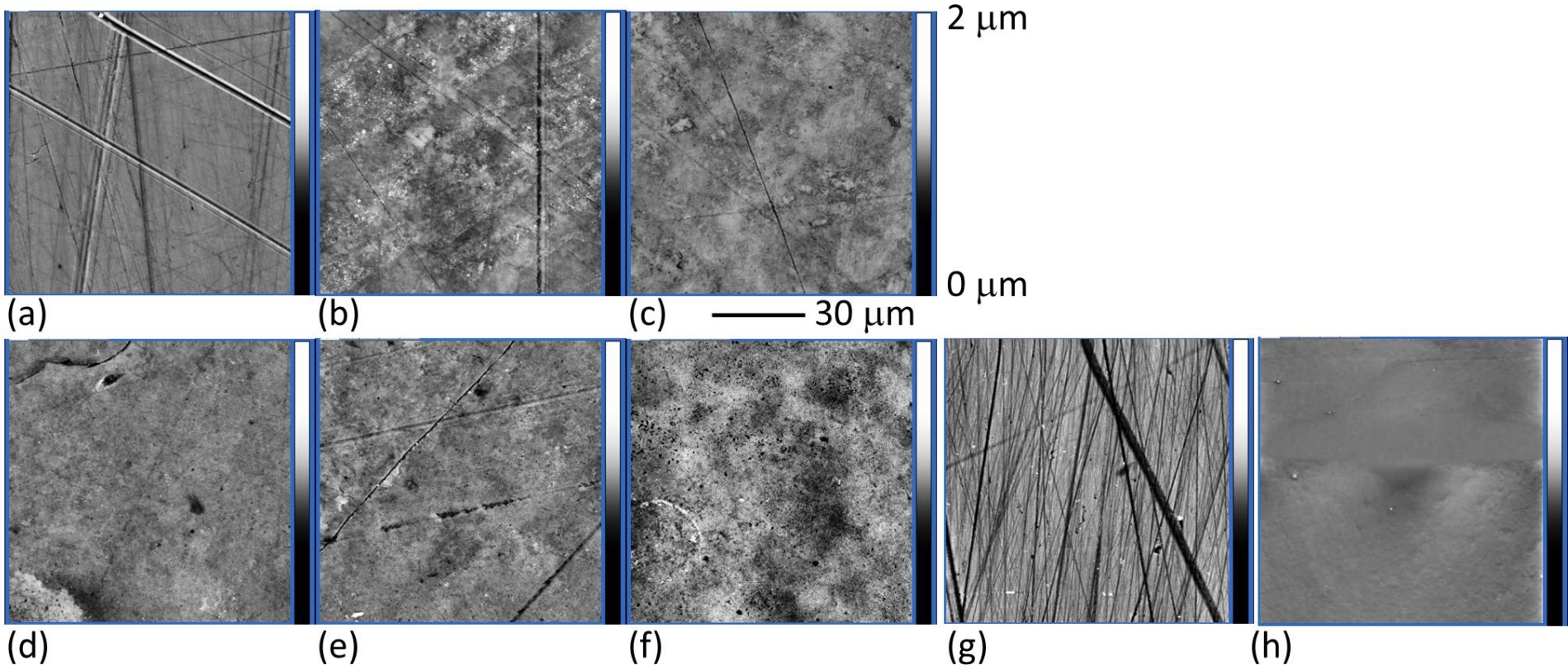

Representative micrographs from AFM scans of veteran and reference lenses. The 90 μm x 90 μm images are shown for: (a) NREL, warehouse; (b) KACST, reference; (c) KACST, Riyadh field 20 y; (d) APS, Phoenix field 27 y; (e) APS, Phoenix, field 22 y; (f) NREL, indoor aged in Ci4000 Weather-ometer for 3 y, M-M lens from APS; (g) KACST, Riyadh reference (after polishing the front surface); and (h) stock PMMA sheet (after removing the protective kraft paper).
All lenses from M-M modules except for (e), obtained from an Intersol module.
For details regarding the weathering (3y cumulative Xe at 60C/60%) of sample (f), see Ref. Miller et. al., SOLMAT, 111, 2013, 165-180.

AFM Data

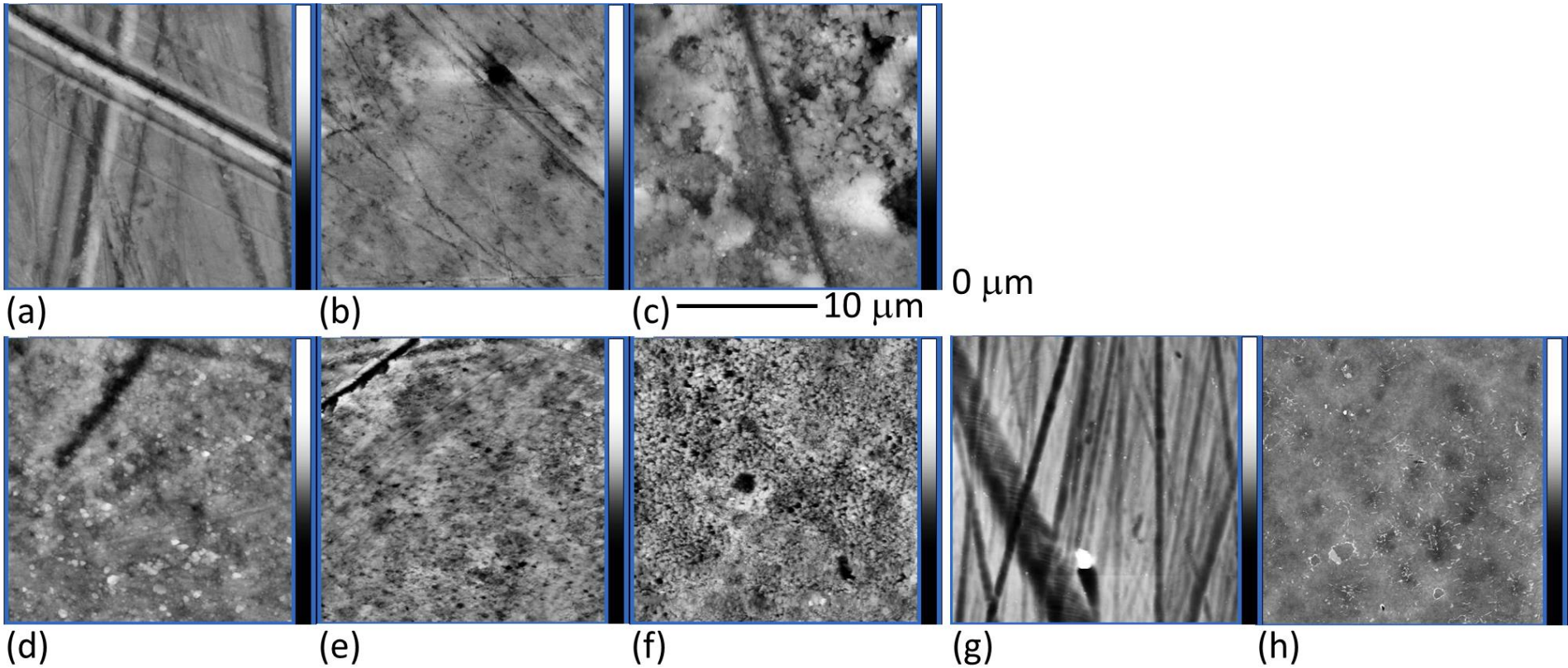

Representative micrographs from AFM scans of veteran and reference lenses. The 20 μm x 20 μm images are shown for: (a) NREL, warehouse; (b) KACST, reference; (c) KACST, Riyadh field 20 y; (d) APS, Phoenix field 27 y; (e) APS, Phoenix, field 22 y; (f) NREL, indoor aged in Ci4000 Weather-ometer for 3 y, M-M lens from APS; (g) KACST, Riyadh reference (after polishing the front surface); and (h) stock PMMA sheet (after removing the protective kraft paper).

All lenses from M-M modules except for (e), obtained from an Intersol module.

For details regarding the weathering (3y cumulative Xe at 60C/60%) of sample (f), see Ref. Miller et. al., SOLMAT, 111, 2013, 165-180.

AFM Data

SITE	SITE LOCATION	SPECIMEN DESIGN	SPECIMEN HISTORY	LENS CLEANING	R_a {nm}	R_{rms} {nm}	R_{pv} {nm}	SCAN SIZE {μm x μm}
NREL	Golden	M-M	warehouse	wet scrubbed	86	118	1,630	90×90
KACST	Riyadh	M-M	reference	spray only	48	62	870	90×90
KACST	Riyadh	M-M	field 20 y	spray only	84	115	1,230	90×90
APS	Phoenix	M-M	field 27 y	spray only/ none	64	85	1,240	90×90
APS	Phoenix	Intersol	field 22 y	none	124	171	1,700	90×90
KACST	Riyadh	M-M	reference	milled + polished	45	64	1,450	90×90
N/A	N/A	N/A	stock PMMA sheet	kraft paper removed	11	16	280	90×90
NREL	Golden	M-M	indoor aged	spray only	47	60	890	90×90

SITE	SITE LOCATION	SPECIMEN DESIGN	SPECIMEN HISTORY	LENS CLEANING	R_a {nm}	R_{rms} {nm}	R_{pv} {nm}	SCAN SIZE {μm x μm}
NREL	Golden	M-M	warehouse	wet scrubbed	64	94	870	20x20
KACST	Riyadh	M-M	reference	spray only	55	72	710	20x20
KACST	Riyadh	M-M	field 20 y	spray only	98	128	590	20x20
APS	Phoenix	M-M	field 27 y	spray only/ none	67	88	880	20x20
APS	Phoenix	Intersol	field 22 y	none	84	112	1,120	20x20
KACST	Riyadh	M-M	reference	milled + polished	48	64	772	20x20
N/A	N/A	N/A	stock PMMA sheet	kraft paper removed	1	2	100	20x20
NREL	Golden	M-M	indoor aged	spray only	40	52	750	20x20

The average (R_a), root-mean-square (R_{rms}), and peak-to-valley (R_{PV}) roughness are reported for the scans. (averaged from 3 separate measurements)

For details regarding the weathering (3y cumulative Xe at 60C/60%) of sample (f), see Ref. Miller et. al., SOLMAT, 111, 2013, 165-180.

SEM: Morphology of 1st Surface

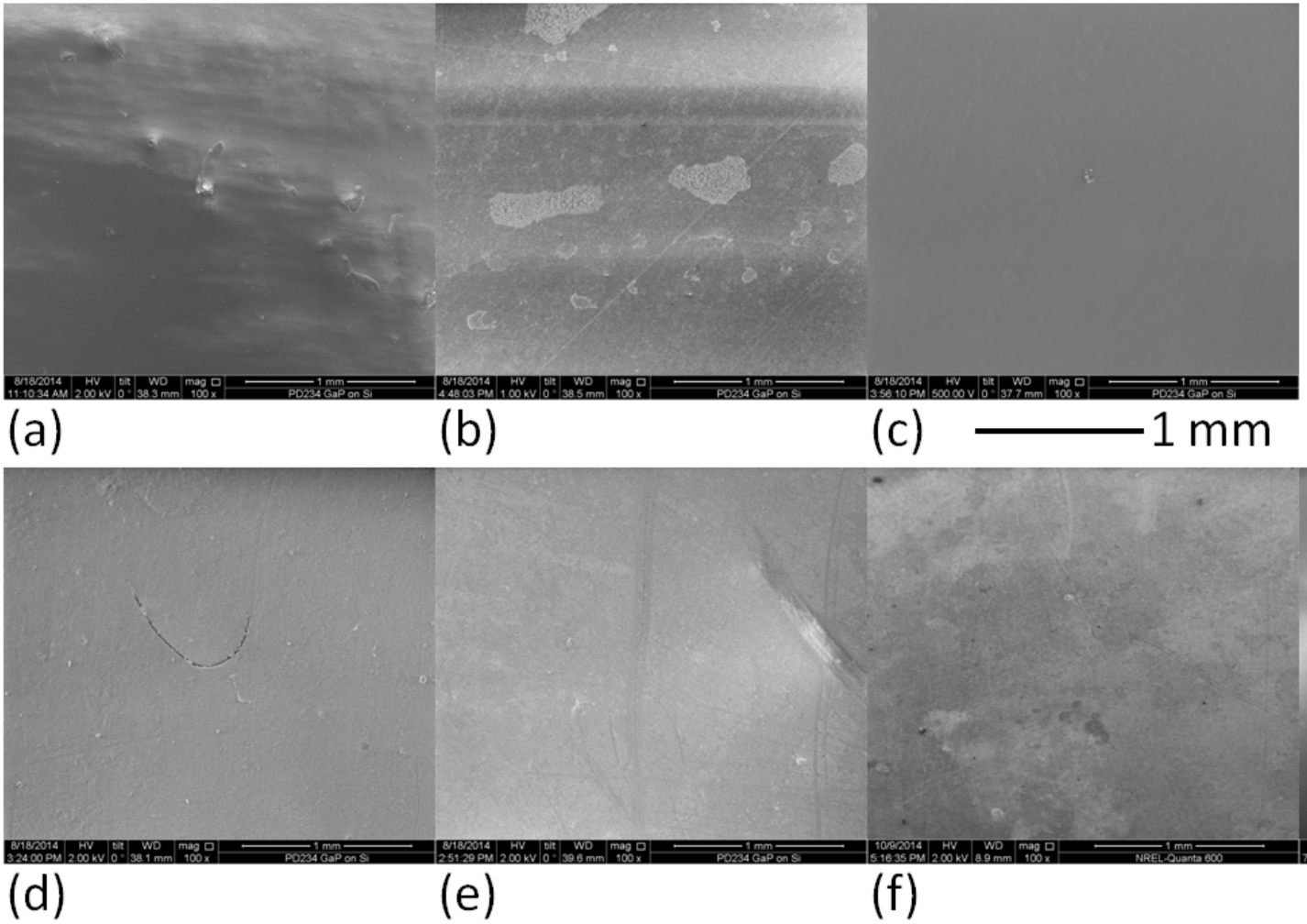

Representative micrographs from SEM scans of veteran and reference lenses. The images, originally obtained at 100x, are shown for: (a) NREL, warehouse; (b) KACST, reference; (c) KACST, Riyadh field 20 y; (d) APS, Phoenix field 27 y; (e) APS, Phoenix, field 22 y; (f) NREL, indoor aged in Ci4000 Weather-ometer for 3 y, M-M lens from APS; and (g) KACST, Riyadh field 20 y (after polishing the front surface).

All lenses from M-M modules except for (e), obtained from an Intersol module.

For details regarding the weathering (3y cumulative Xe at 60C/60%) of sample (f), see Ref. Miller et. al., SOLMAT, 111, 2013, 165-180.

SEM: Morphology of 1st Surface

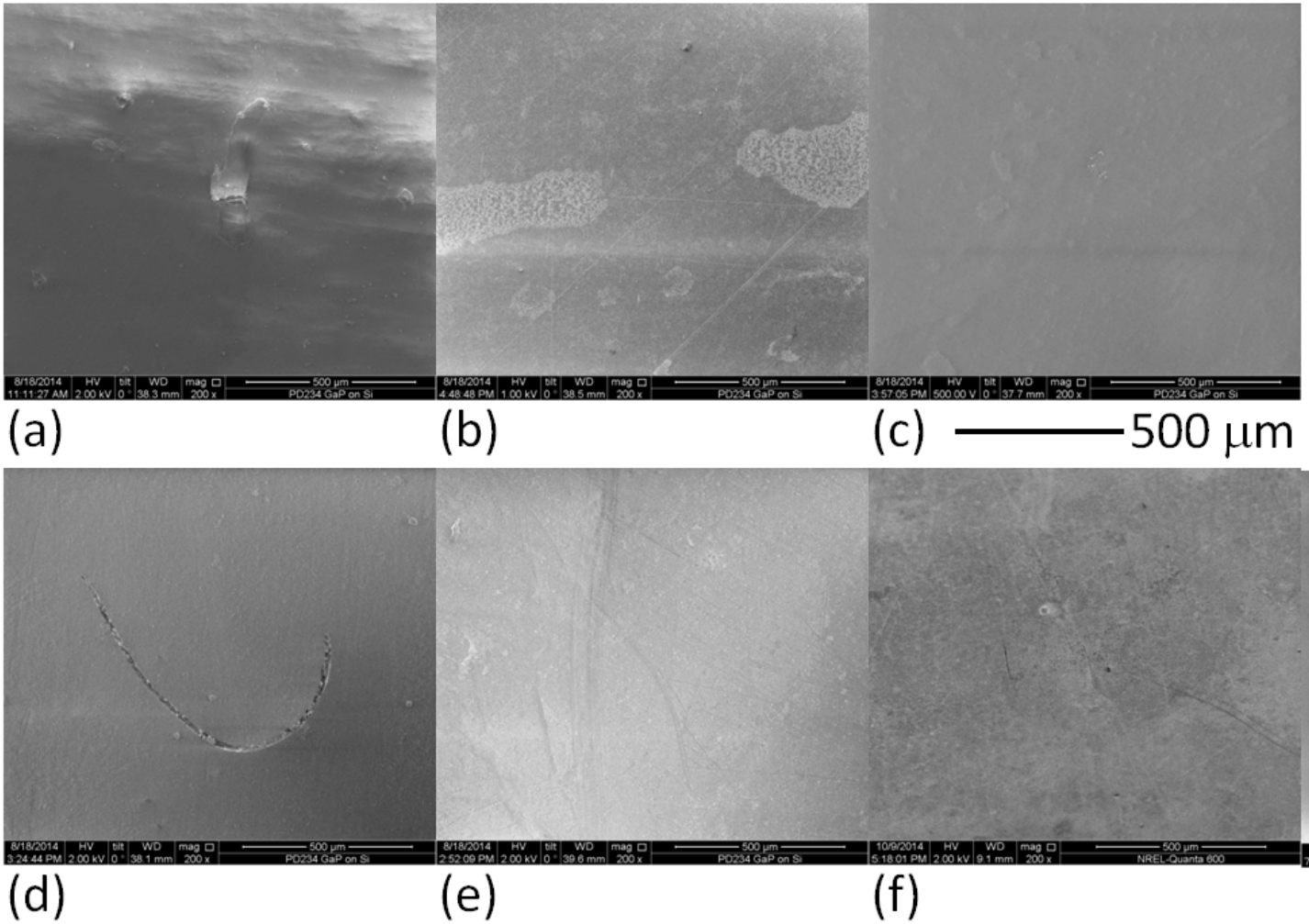

Representative micrographs from SEM scans of veteran and reference lenses. The images, originally obtained at 200x, are shown for: (a) NREL, warehouse; (b) KACST, reference; (c) KACST, Riyadh field 20 y; (d) APS, Phoenix field 27 y; (e) APS, Phoenix, field 22 y; (f) NREL, indoor aged in Ci4000 Weather-ometer for 3 y, M-M lens from APS; and (g) KACST, Riyadh field 20 y (after polishing the front surface).

All lenses from M-M modules except for (e), obtained from an Intersol module.

For details regarding the weathering of sample (f), see Ref. Miller et. al., SOLMAT, 111, 2013, 165-180.

SEM: Morphology of 1st Surface

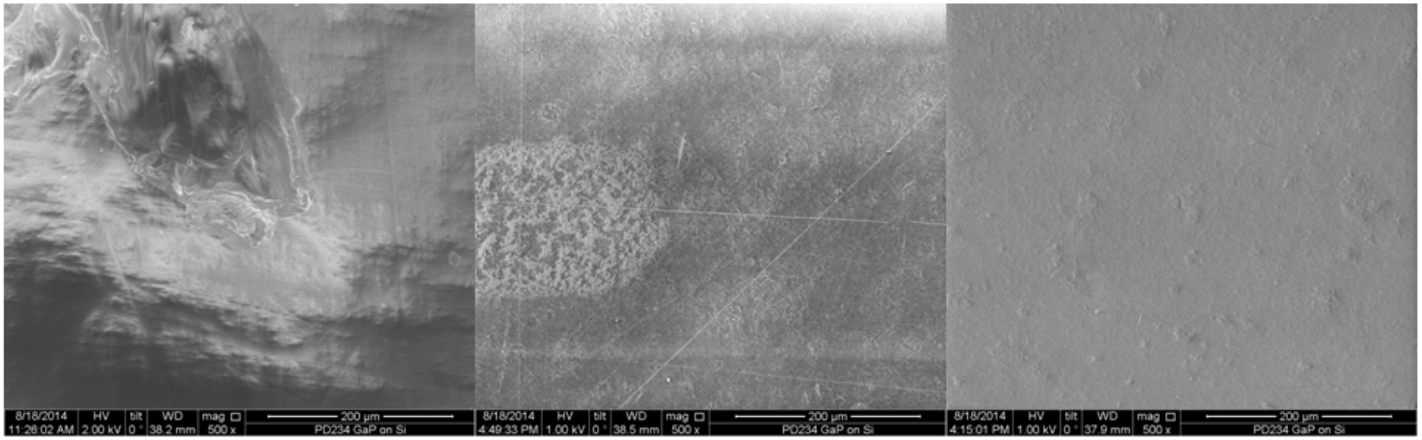

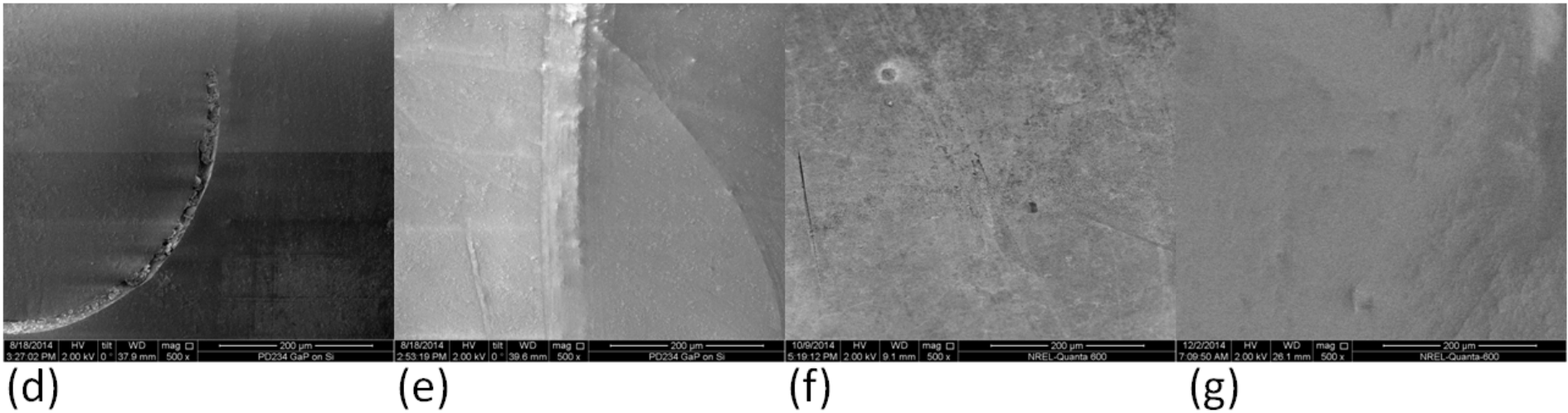

Representative micrographs from SEM scans of veteran and reference lenses. The images, originally obtained at 500x, are shown for: (a) NREL, warehouse; (b) KACST, reference; (c) KACST, Riyadh field 20 y; (d) APS, Phoenix field 27 y; (e) APS, Phoenix, field 22 y; (f) NREL, indoor aged in Ci4000 Weather-ometer for 3 y, M-M lens from APS; and (g) KACST, Riyadh field 20 y (after polishing the front surface).

All lenses from M-M modules except for (e), obtained from an Intersol module.

For details regarding the weathering of sample (f), see Ref. Miller et. al., SOLMAT, 111, 2013, 165-180.

SEM: Morphology of 1st Surface

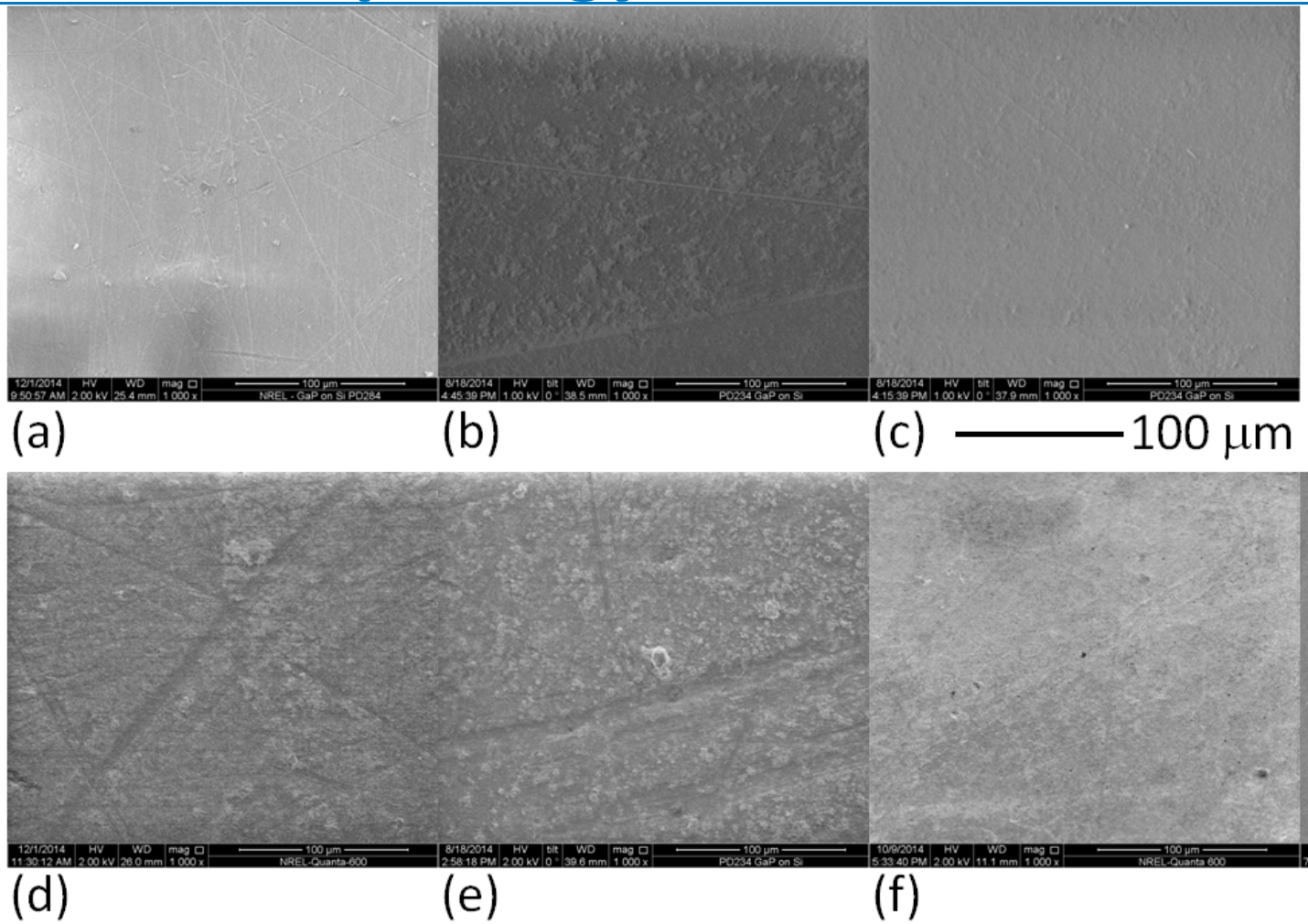

Representative micrographs from SEM scans of veteran and reference lenses. The images, originally obtained at 1,000x, are shown for: (a) NREL, warehouse; (b) KACST, reference; (c) KACST, Riyadh field 20 y; (d) APS, Phoenix field 27 y; (e) APS, Phoenix, field 22 y; (f) NREL, indoor aged in Ci4000 Weather-ometer for 3 y, M-M lens from APS; and (g) KACST, Riyadh field 20 y (after polishing the front surface).

All lenses from M-M modules except for (e), obtained from an Intersol module.

For details regarding the weathering (3y cumulative Xe at 60C/60%) of sample (f), see Ref. Miller et. al., SOLMAT, 111, 2013, 165-180.

SEM: Morphology of 1st Surface

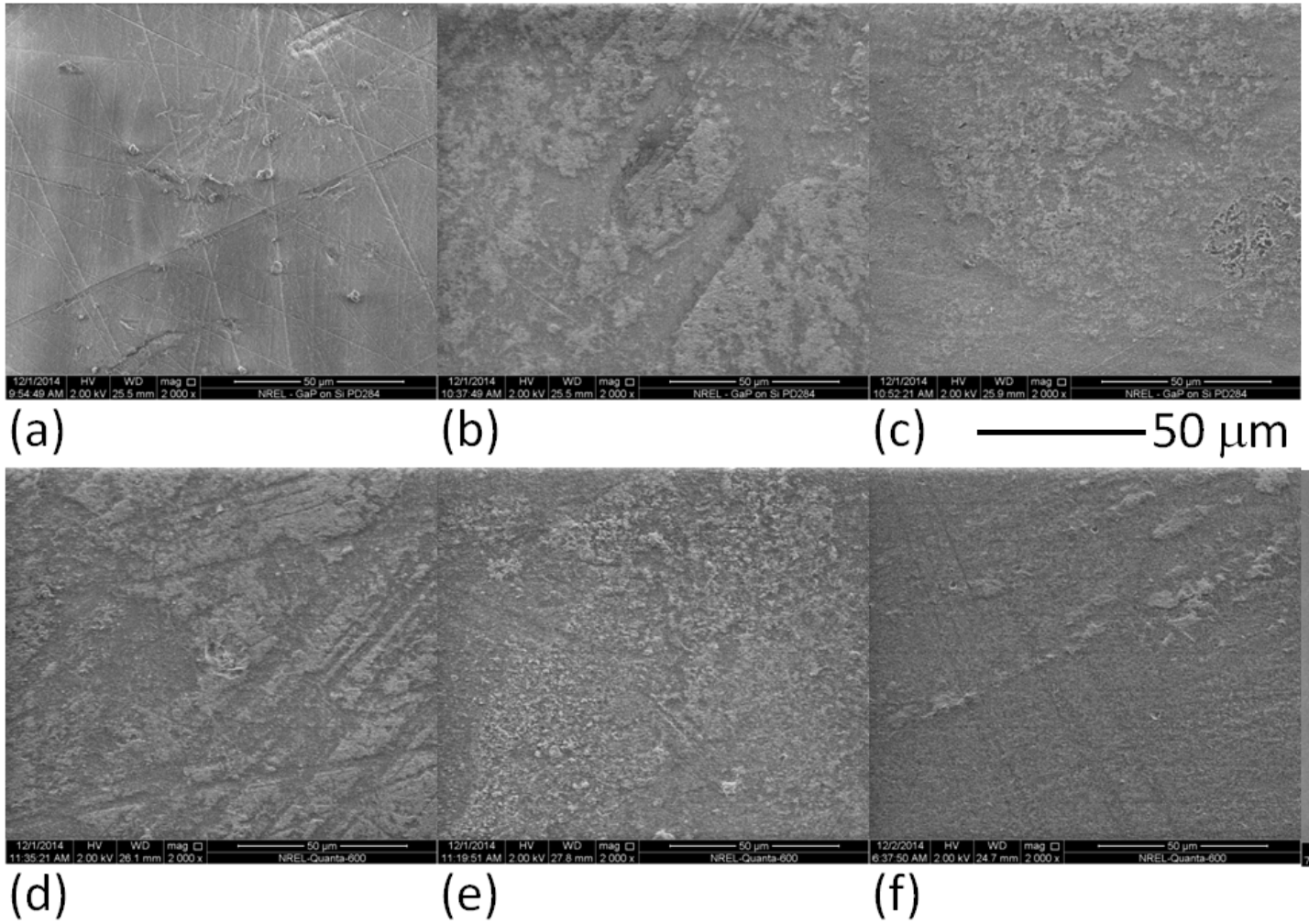

Representative micrographs from SEM scans of veteran and reference lenses. The images, originally obtained at 2,000x, are shown for: (a) NREL, warehouse; (b) KACST, reference; (c) KACST, Riyadh field 20 y; (d) APS, Phoenix field 27 y; (e) APS, Phoenix, field 22 y; (f) NREL, indoor aged in Ci4000 Weather-ometer for 3 y, M-M lens from APS; and (g) KACST, Riyadh field 20 y (after polishing the front surface).

All lenses from M-M modules except for (e), obtained from an Intersol module.

For details regarding the weathering (3y cumulative Xe at 60C/60%) of sample (f), see Ref. Miller et. al., SOLMAT, 111, 2013, 165-180.

SEM: Morphology of 1st Surface

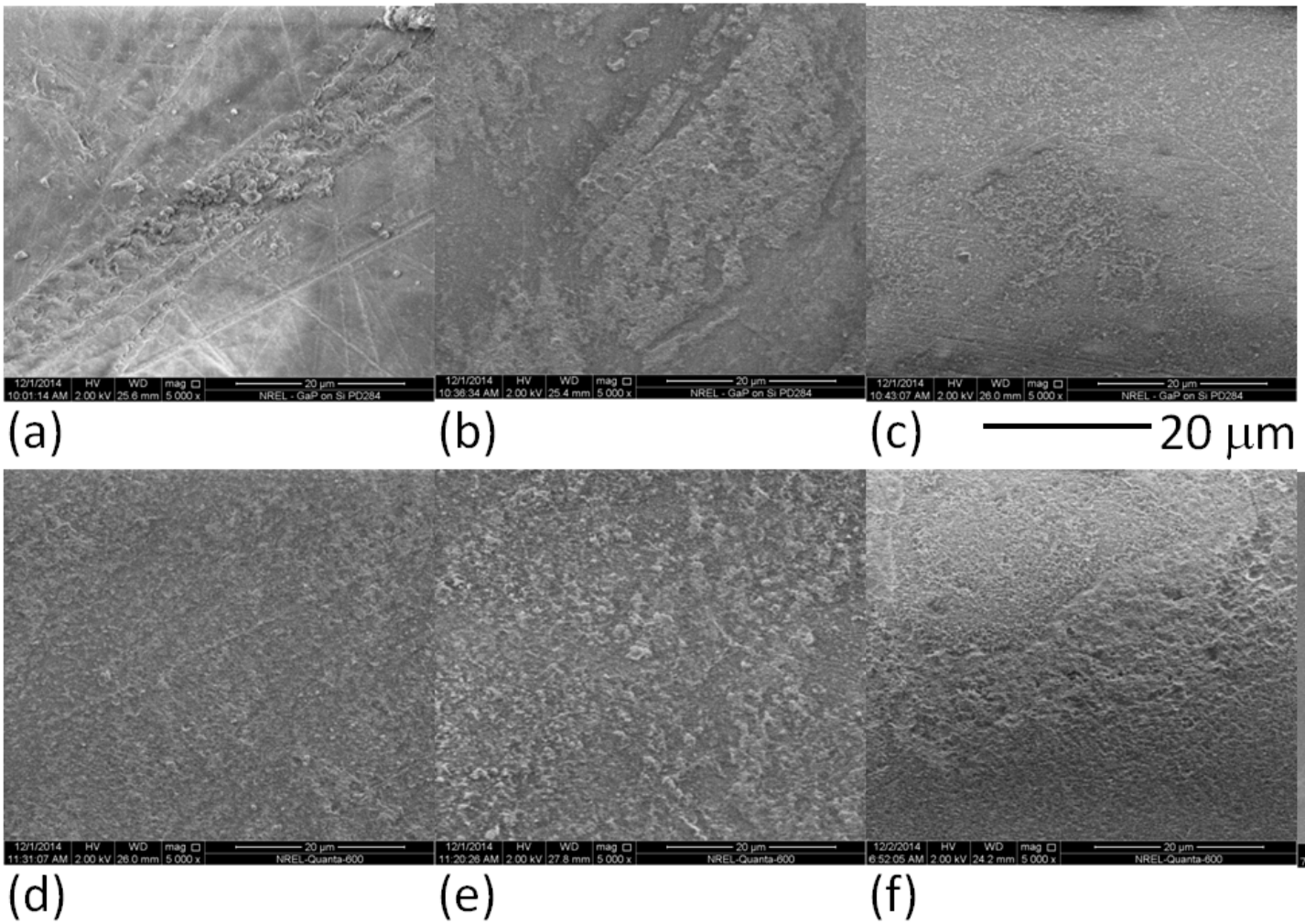

Representative micrographs from SEM scans of veteran and reference lenses. The images, originally obtained at 5,000x, are shown for: (a) NREL, warehouse; (b) KACST, reference; (c) KACST, Riyadh field 20 y; (d) APS, Phoenix field 27 y; (e) APS, Phoenix, field 22 y; (f) NREL, indoor aged in Ci4000 Weather-ometer for 3 y, M-M lens from APS; and (g) KACST, Riyadh field 20 y (after polishing the front surface).

All lenses from M-M modules except for (e), obtained from an Intersol module.

For details regarding the weathering (3y cumulative Xe at 60C/60%) of sample (f), see Ref. Miller et. al., SOLMAT, 111, 2013, 165-180.

SEM: Morphology of 1st Surface

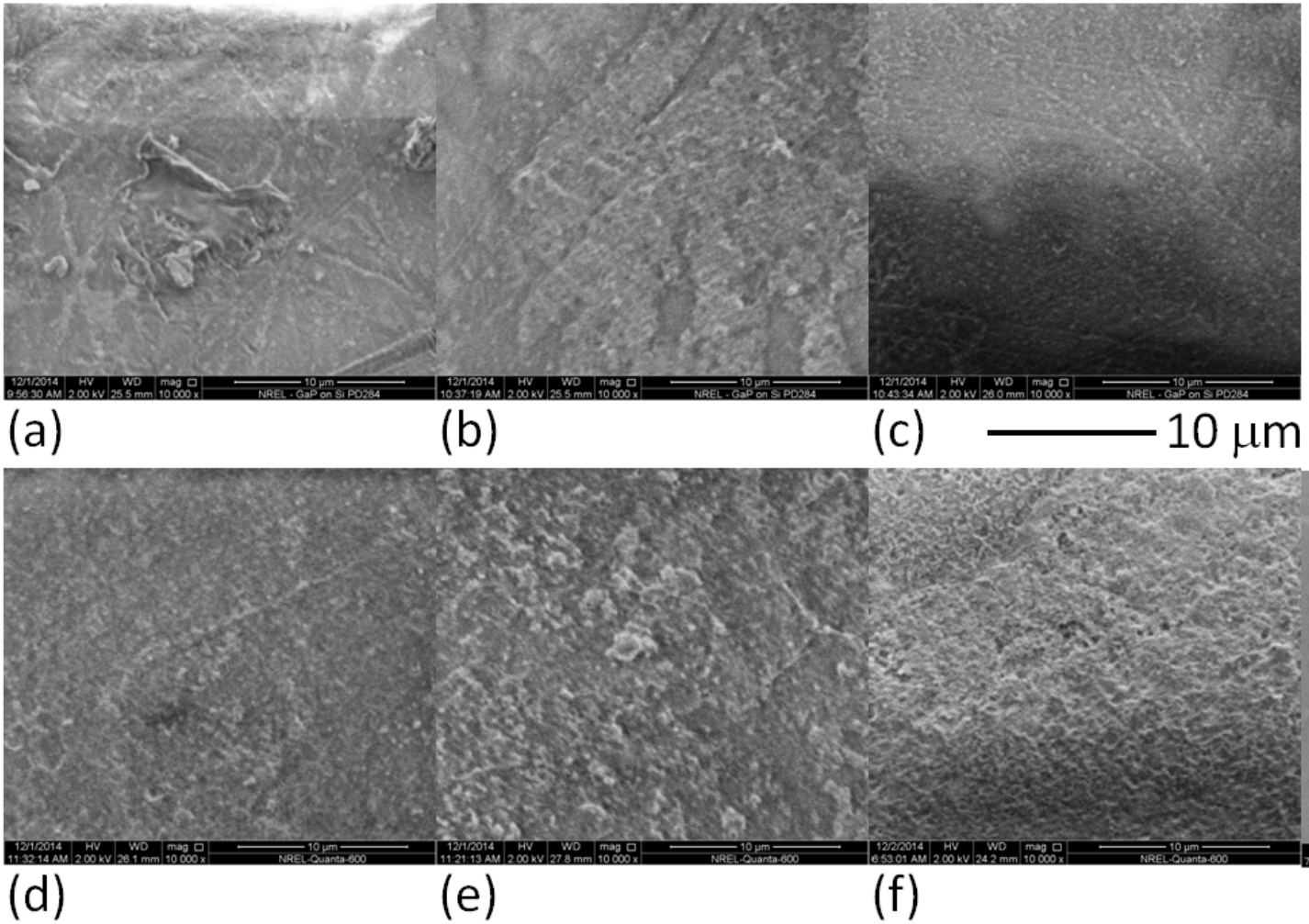

Representative micrographs from SEM scans of veteran and reference lenses. The images, originally obtained at 10,000x, are shown for: (a) NREL, warehouse; (b) KACST, reference; (c) KACST, Riyadh field 20 y; (d) APS, Phoenix field 27 y; (e) APS, Phoenix, field 22 y; (f) NREL, indoor aged in Ci4000 Weather-ometer for 3 y, M-M lens from APS; and (g) KACST, Riyadh field 20 y (after polishing the front surface).

All lenses from M-M modules except for (e), obtained from an Intersol module.

For details regarding the weathering (3y cumulative Xe at 60C/60%) of sample (f), see Ref. Miller et. al., SOLMAT, 111, 2013, 165-180.

Cross-Sectional SEM: Subsurface Integrity (1st Surface)

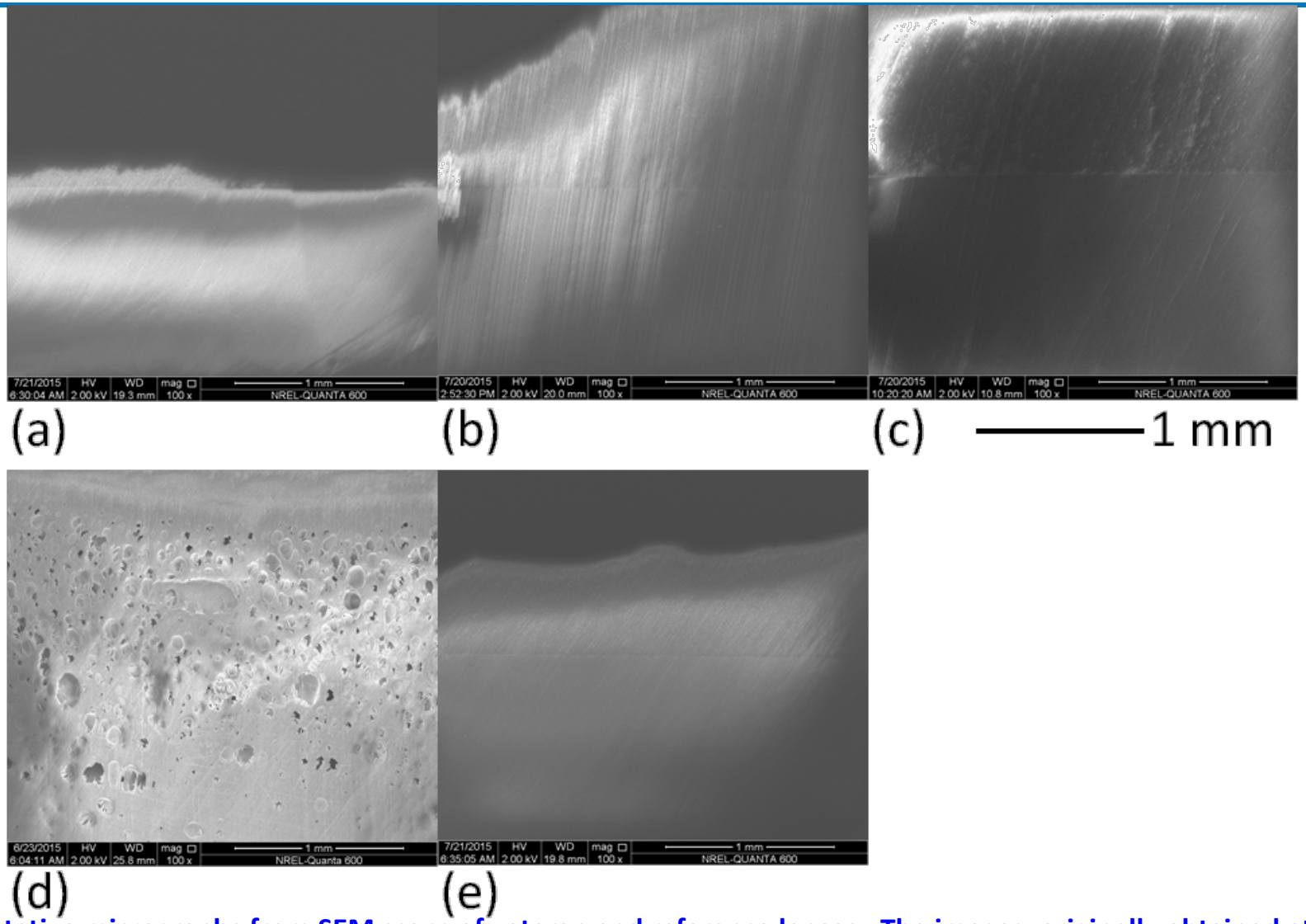

Representative micrographs from SEM scans of veteran and reference lenses. The images, originally obtained at 100x, are shown for: (a) NREL, warehouse; (b) KACST, reference; (c) KACST, Riyadh field 20 y; (d) APS, Phoenix field 27 y; (e) APS, Phoenix, field 22 y.

All lenses from M-M modules except for (e), obtained from an Intersol module.

Cross-Sectional SEM: Subsurface Integrity (1st Surface)

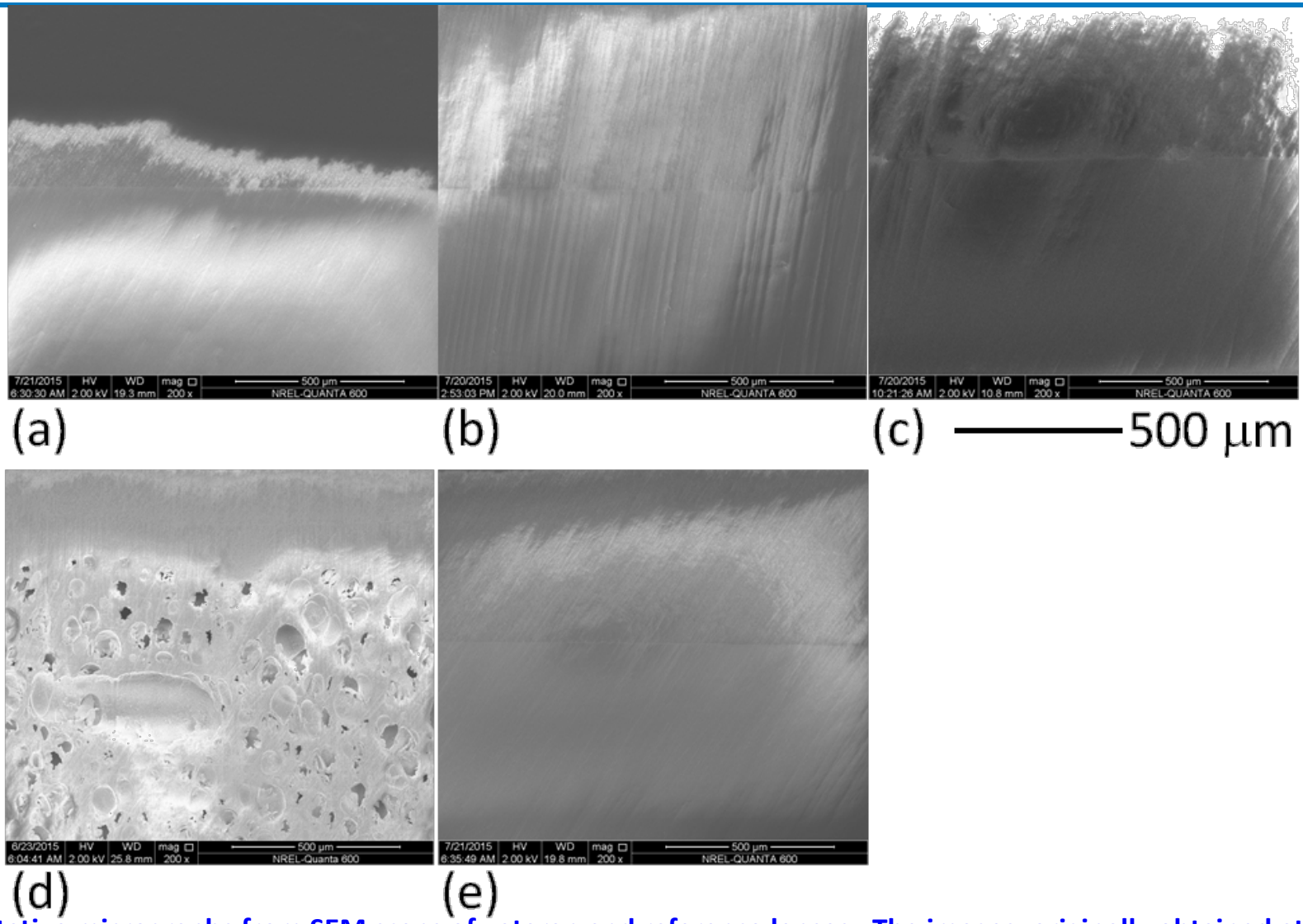

Representative micrographs from SEM scans of veteran and reference lenses. The images, originally obtained at 200x, are shown for: (a) NREL, warehouse; (b) KACST, reference; (c) KACST, Riyadh field 20 y; (d) APS, Phoenix field 27 y; (e) APS, Phoenix, field 22 y.

All lenses from M-M modules except for (e), obtained from an Intersol module.

Cross-Sectional SEM: Subsurface Integrity (1st Surface)

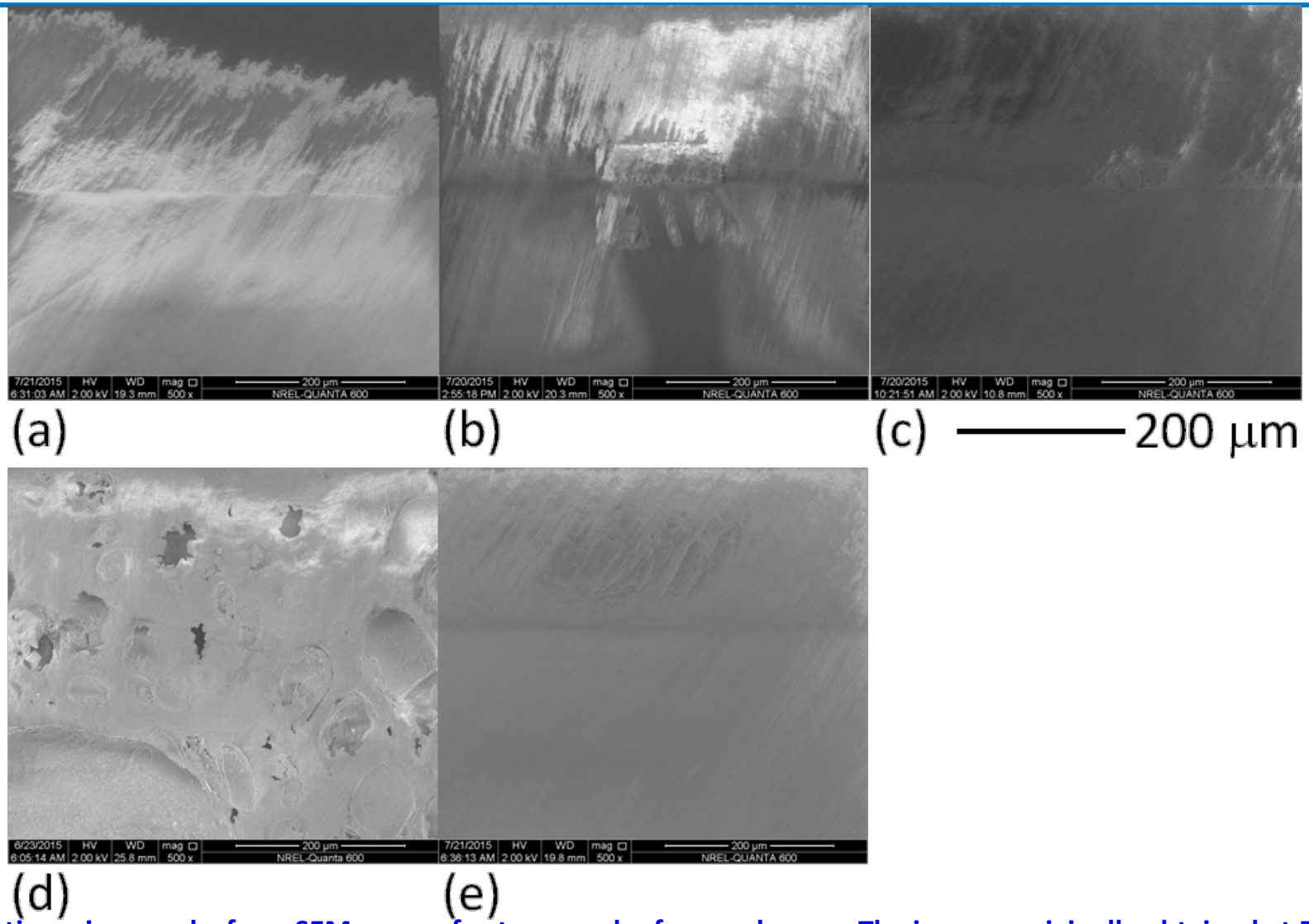

Representative micrographs from SEM scans of veteran and reference lenses. The images, originally obtained at 500x, are shown for: (a) NREL, warehouse; (b) KACST, reference; (c) KACST, Riyadh field 20 y; (d) APS, Phoenix field 27 y; (e) APS, Phoenix, field 22 y.

All lenses from M-M modules except for (e), obtained from an Intersol module.

Cross-Sectional SEM: Subsurface Integrity (1st Surface)

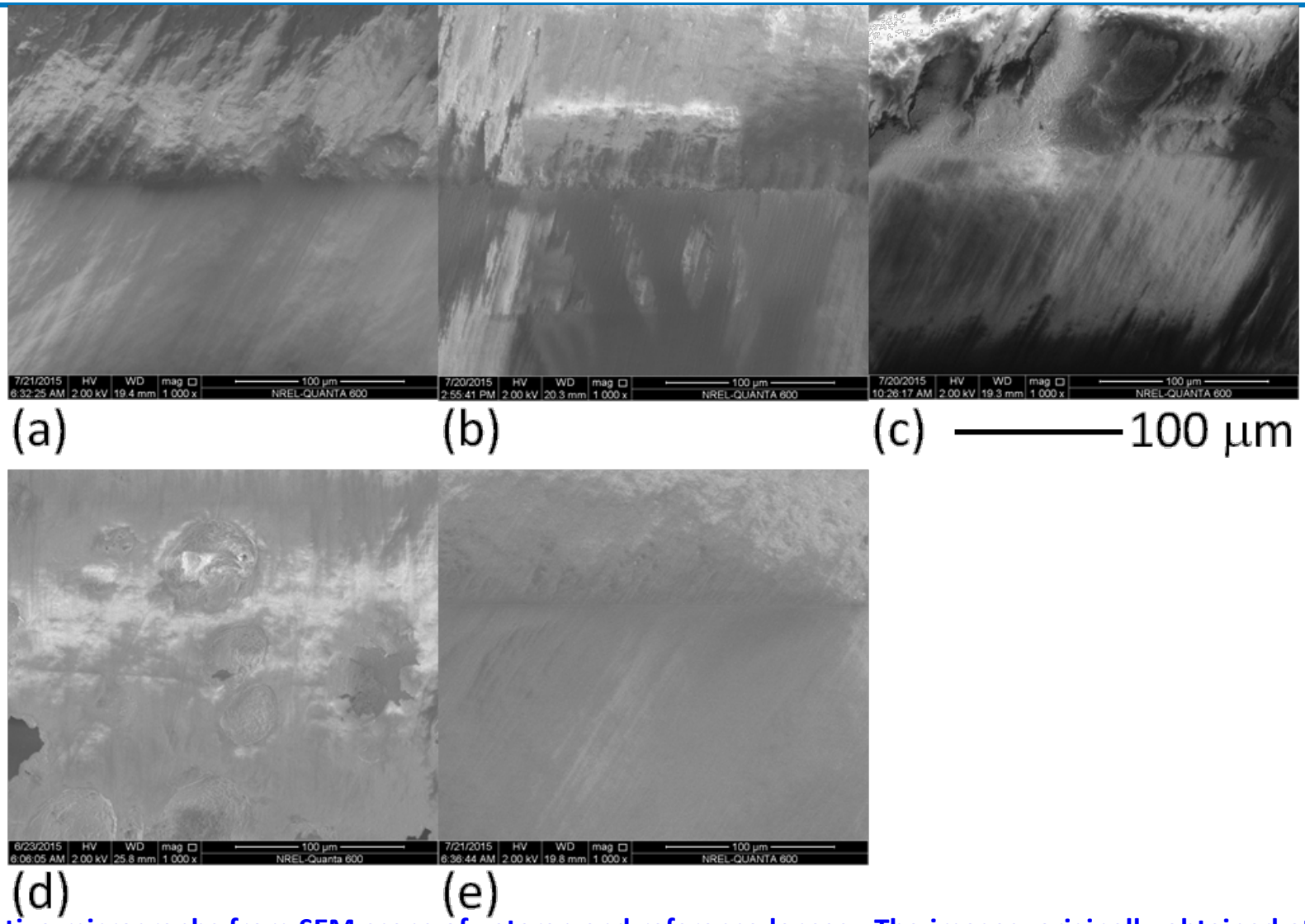

Representative micrographs from SEM scans of veteran and reference lenses. The images, originally obtained at 1,000x, are shown for: (a) NREL, warehouse; (b) KACST, reference; (c) KACST, Riyadh field 20 y; (d) APS, Phoenix field 27 y; (e) APS, Phoenix, field 22 y.

All lenses from M-M modules except for (e), obtained from an Intersol module.

Cross-Sectional SEM: Subsurface Integrity (1st Surface)

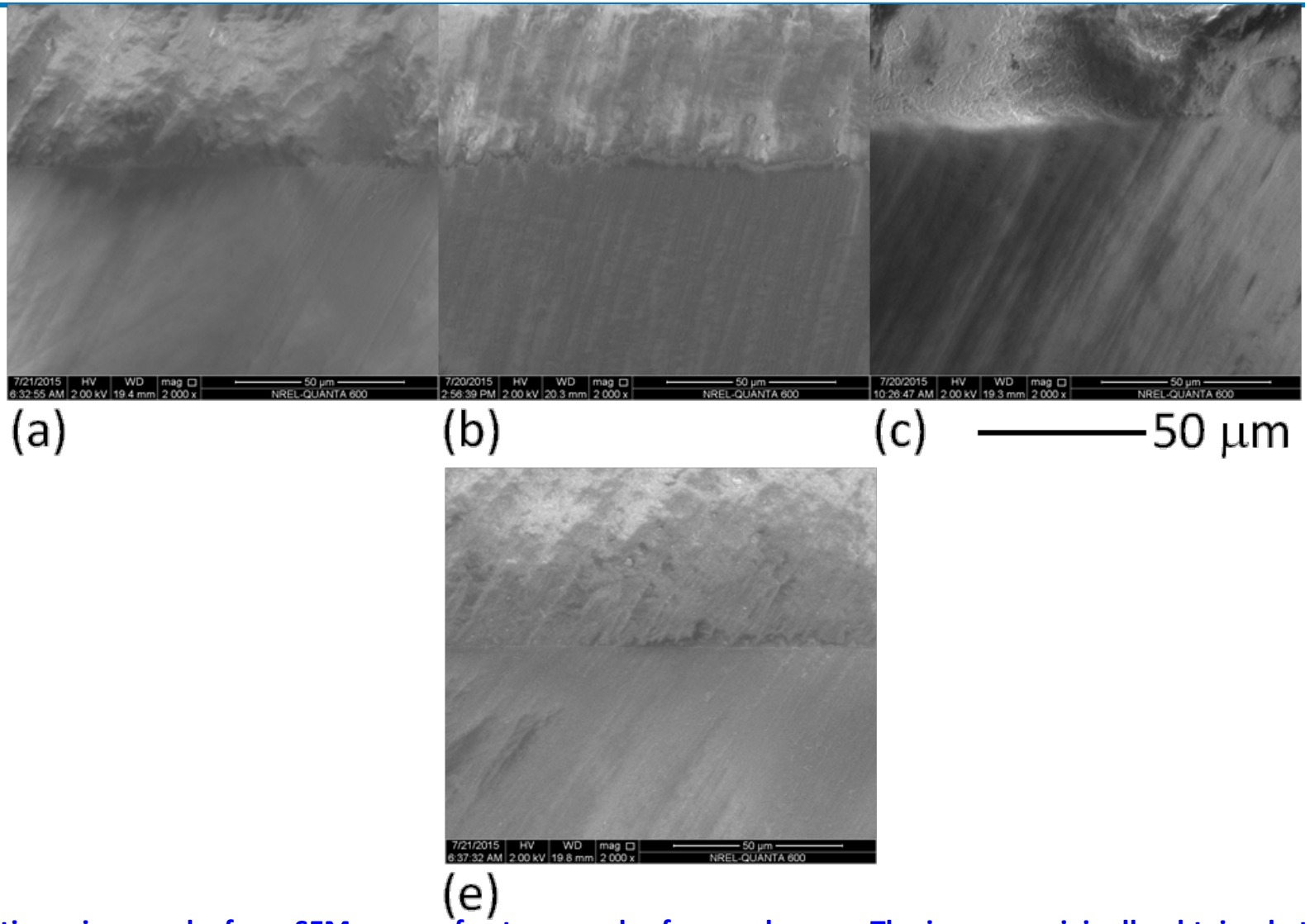

Representative micrographs from SEM scans of veteran and reference lenses. The images, originally obtained at 2,000x, are shown for: (a) NREL, warehouse; (b) KACST, reference; (c) KACST, Riyadh field 20 y; (d) APS, Phoenix field 27 y; (e) APS, Phoenix, field 22 y.

All lenses from M-M modules except for (e), obtained from an Intersol module.

Cross-Sectional Microscopy: Subsurface Integrity (1st Surface)

(a) (b) 1 mm

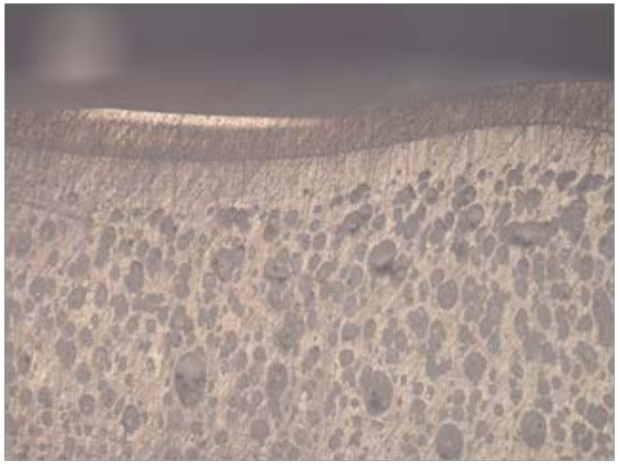

(d)

Representative micrographs from optical images of veteran and reference lenses. The images, originally obtained at 50x, are shown for: (a) NREL, warehouse; (b) KACST, reference; (c) KACST, Riyadh field 20 y; (d) APS, Phoenix field 27 y; (e) APS, Phoenix, field 22 y. The color during imaging was set to show maximum image contrast, using a polarizer.
All lenses from M-M modules except for (e), obtained from an Intersol module.

Cross-Sectional Microscopy: Subsurface Integrity (1st Surface)

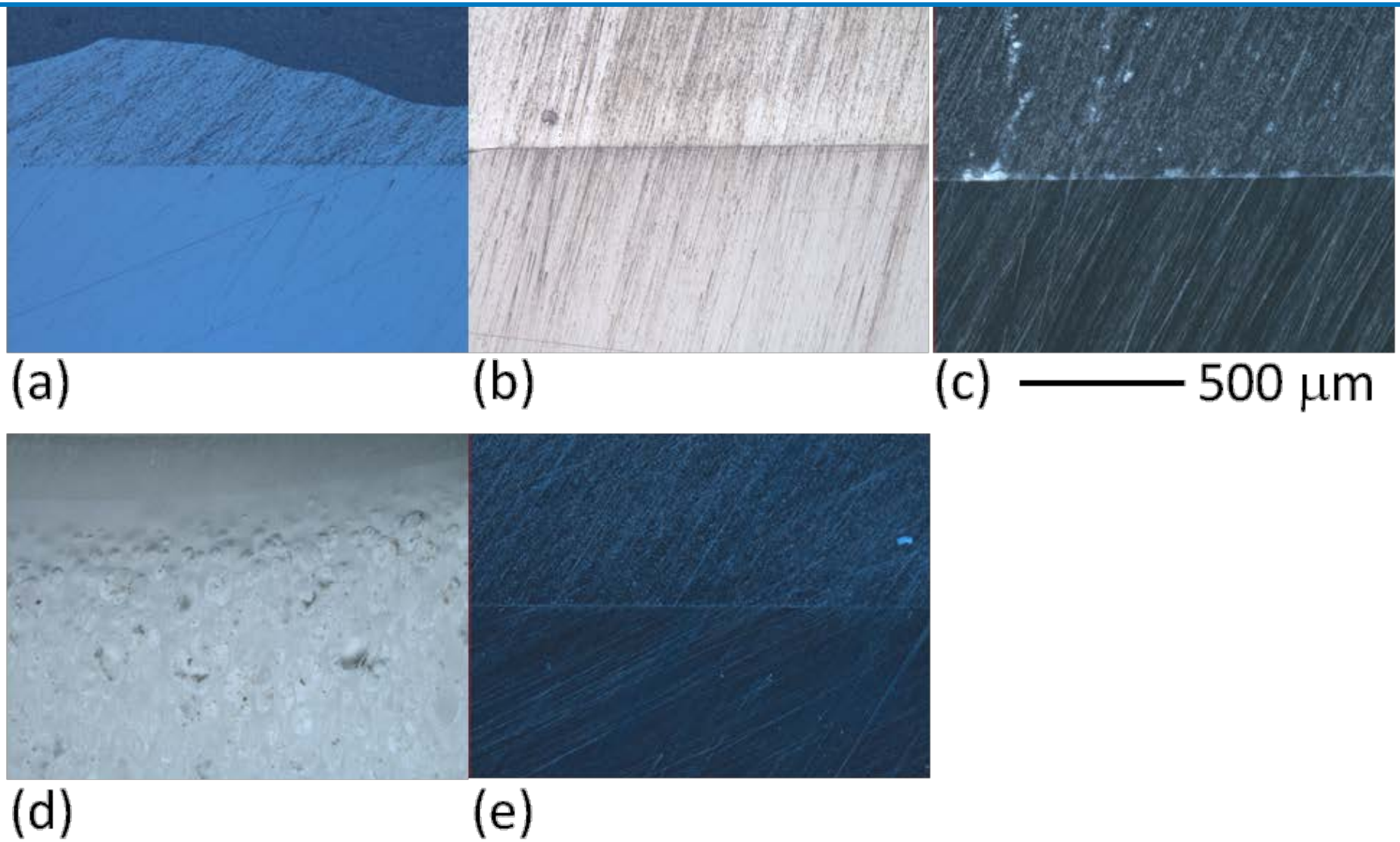

Representative micrographs from optical images of veteran and reference lenses. The images, originally obtained at 100x, are shown for: (a) NREL, warehouse; (b) KACST, reference; (c) KACST, Riyadh field 20 y; (d) APS, Phoenix field 27 y; (e) APS, Phoenix, field 22 y. The color during imaging was set to show maximum image contrast, using a polarizer. All lenses from M-M modules except for (e), obtained from an Intersol module.

Cross-Sectional Microscopy: Subsurface Integrity (1st Surface)

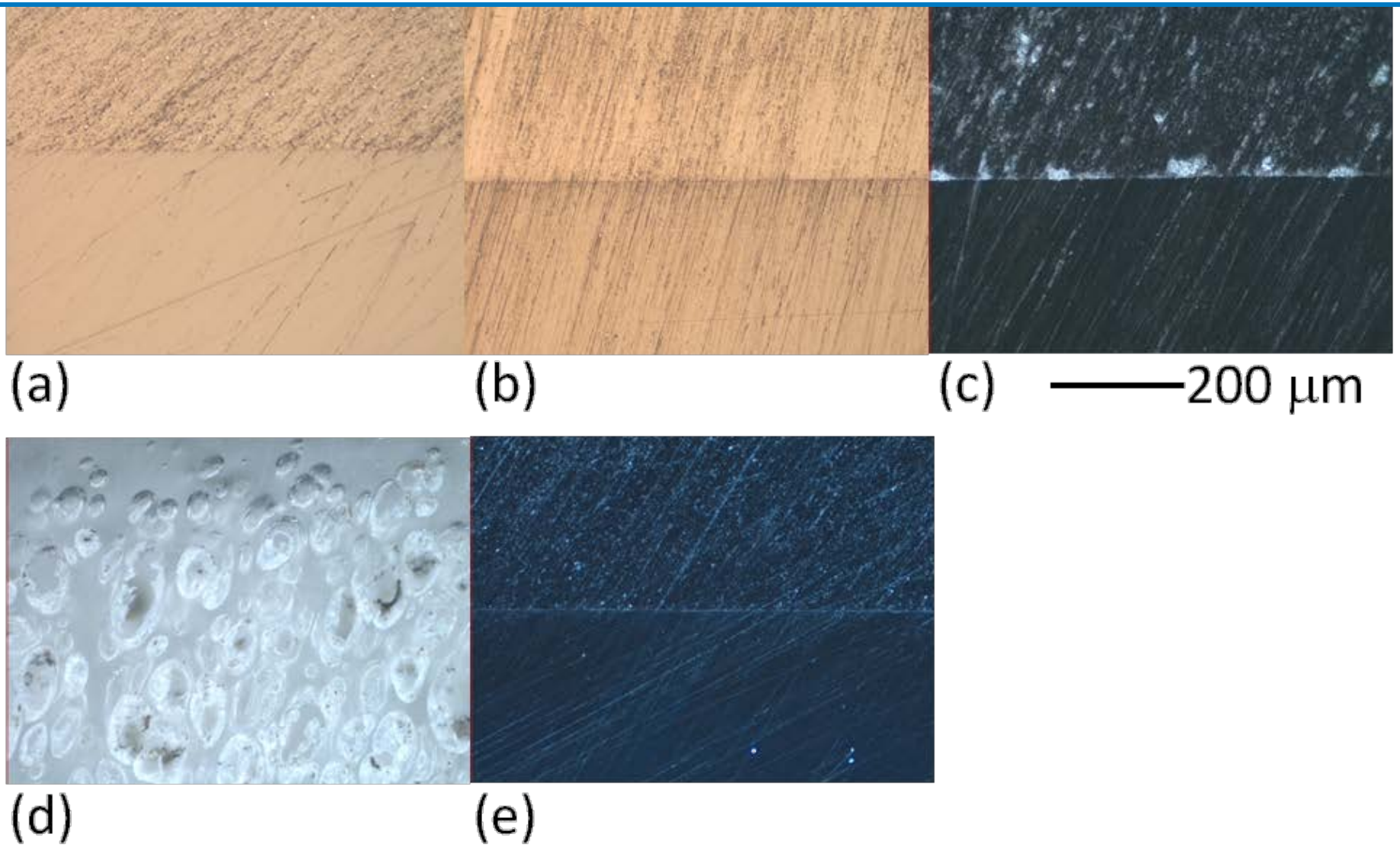

Representative micrographs from optical images of veteran and reference lenses. The images, originally obtained at 200x, are shown for: (a) NREL, warehouse; (b) KACST, reference; (c) KACST, Riyadh field 20 y; (d) APS, Phoenix field 27 y; (e) APS, Phoenix, field 22 y. The color during imaging was set to show maximum image contrast, using a polarizer. All lenses from M-M modules except for (e), obtained from an Intersol module.

Cross-Sectional Microscopy: Subsurface Integrity (1st Surface)

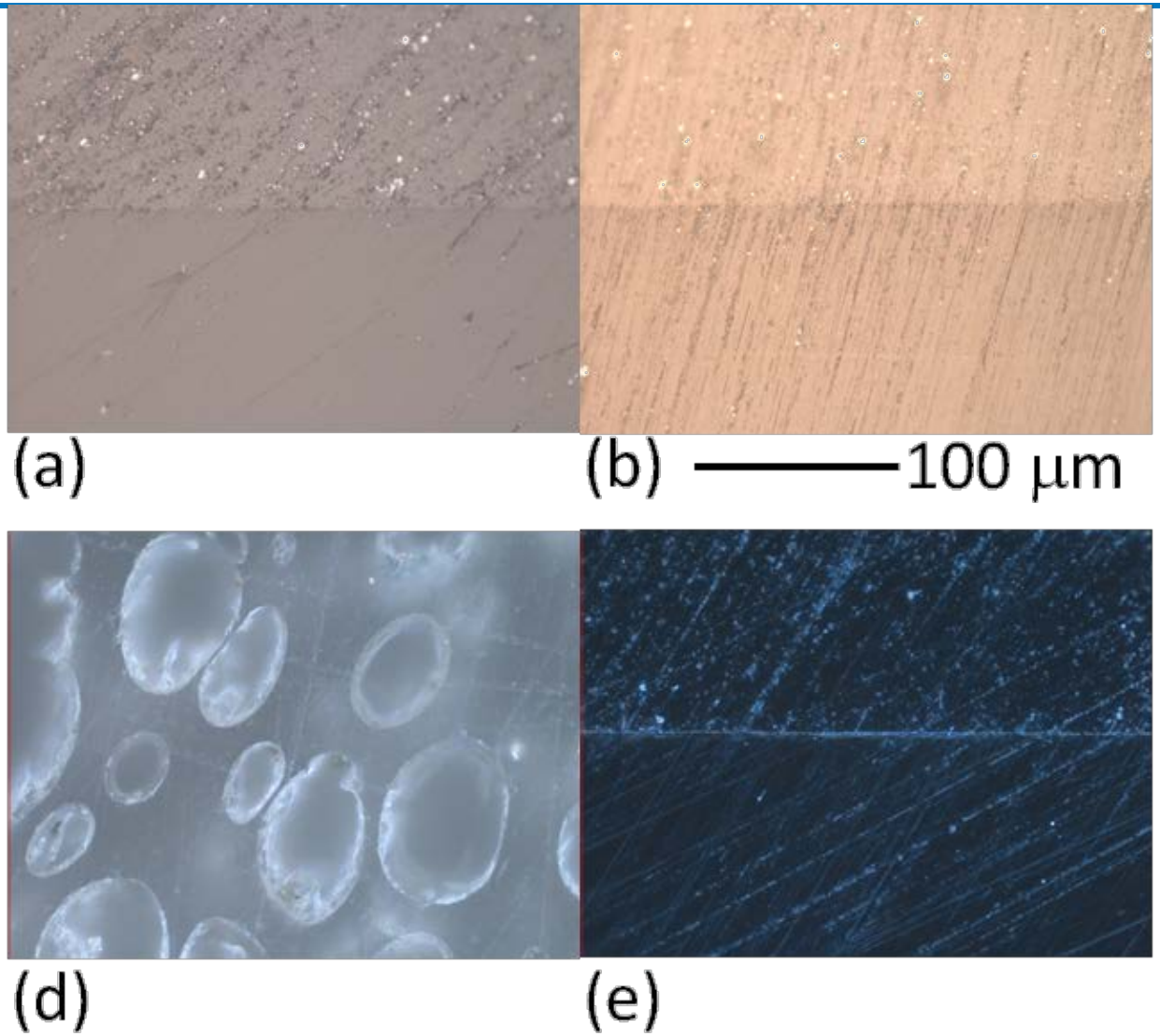

Representative micrographs from optical images of veteran and reference lenses. The images, originally obtained at 500x, are shown for: (a) NREL, warehouse; (b) KACST, reference; (c) KACST, Riyadh field 20 y; (d) APS, Phoenix field 27 y; (e) APS, Phoenix, field 22 y. The color during imaging was set to show maximum image contrast, using a polarizer.
All lenses from M-M modules except for (e), obtained from an Intersol module.

Cross-Sectional Microscopy: Facet Tip Geometry

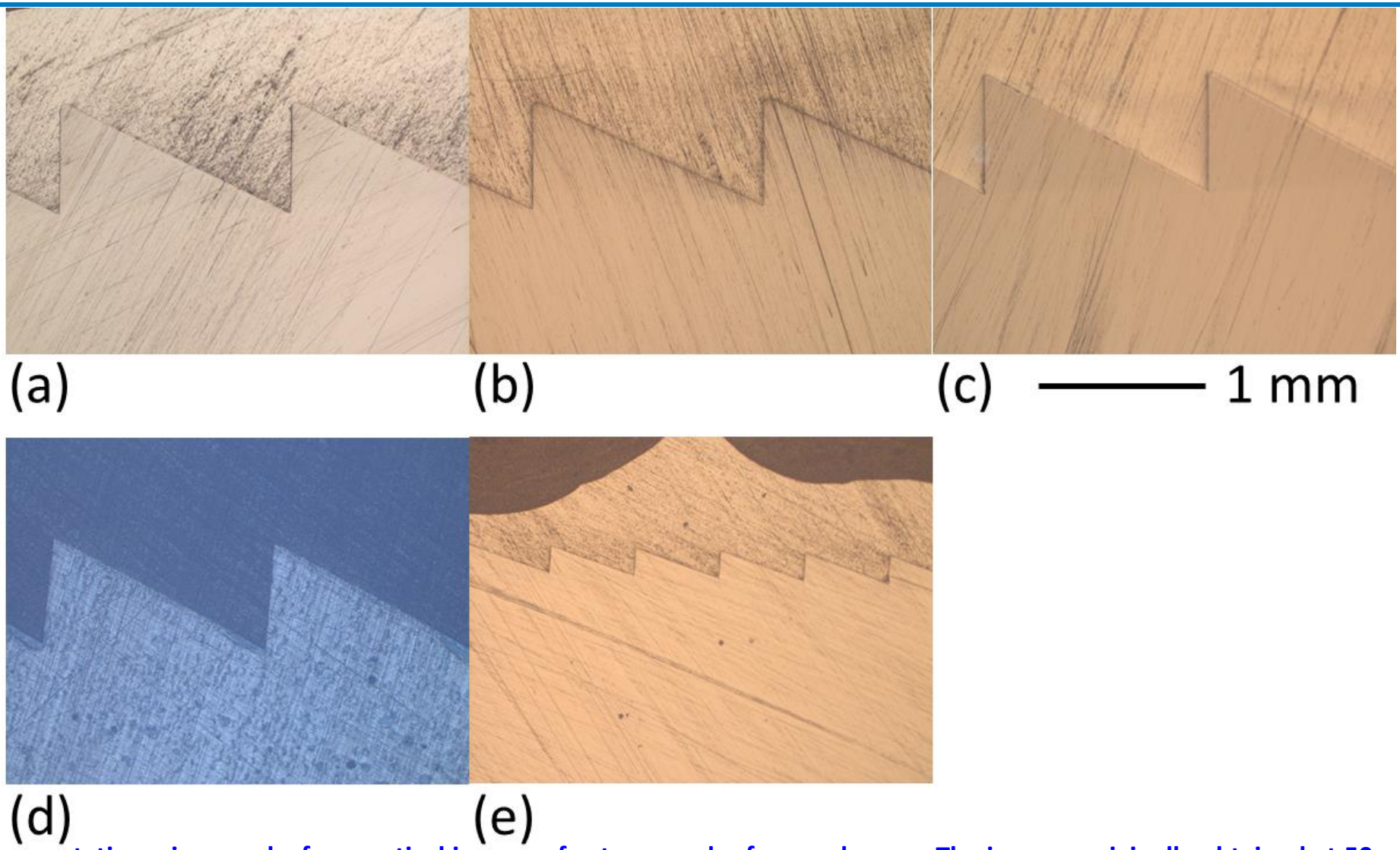

Representative micrographs from optical images of veteran and reference lenses. The images, originally obtained at 50x, are shown for: (a) NREL, warehouse; (b) KACST, reference; (c) KACST, Riyadh field 20 y; (d) APS, Phoenix field 27 y; (e) APS, Phoenix, field 22 y. The color during imaging was set to show maximum image contrast, using a polarizer.
All lenses from M-M modules except for (e), obtained from an Intersol module.

Cross-Sectional Microscopy: Facet Tip Geometry

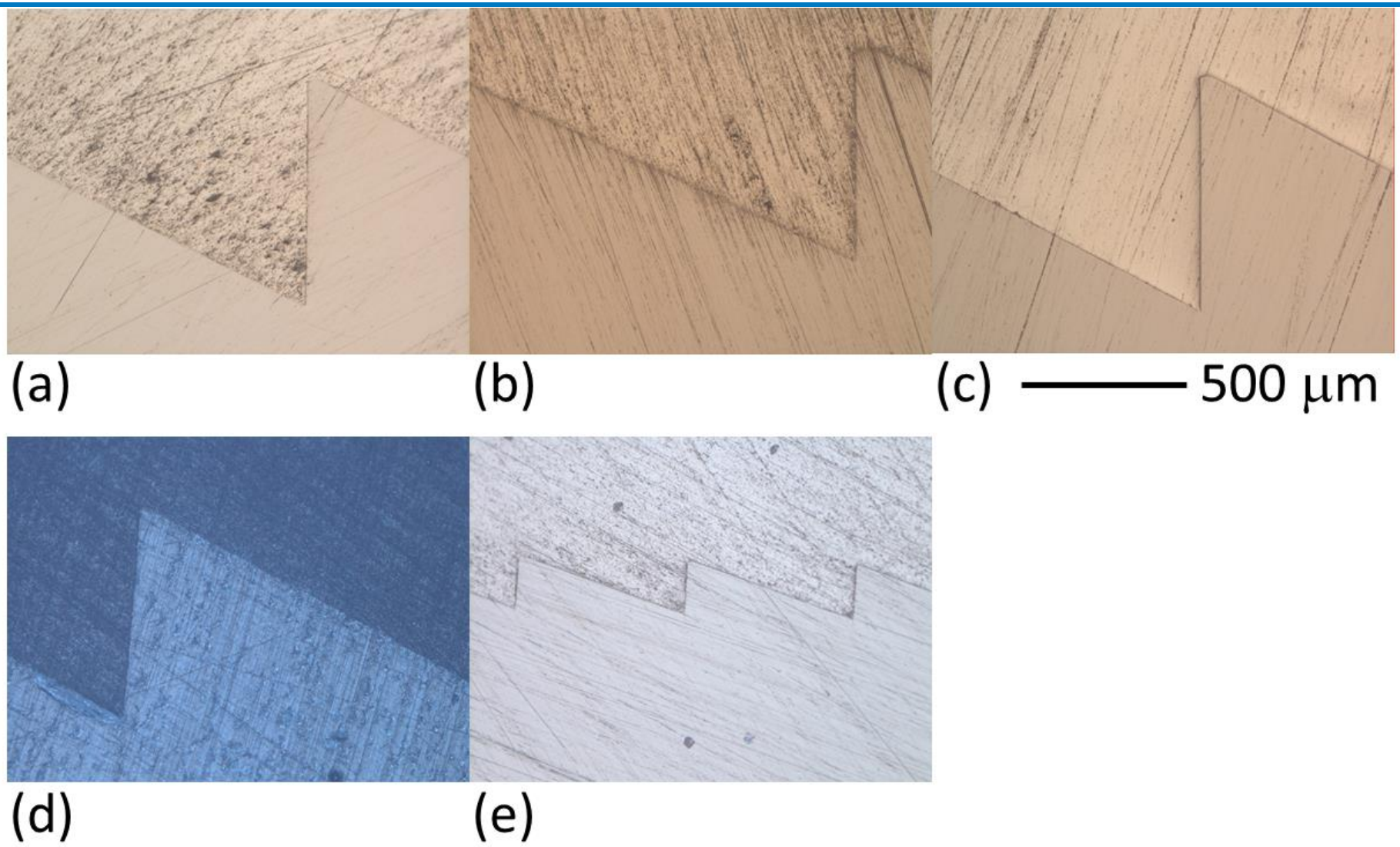

Representative micrographs from optical images of veteran and reference lenses. The images, originally obtained at 100x, are shown for: (a) NREL, warehouse; (b) KACST, reference; (c) KACST, Riyadh field 20 y; (d) APS, Phoenix field 27 y; (e) APS, Phoenix, field 22 y. The color during imaging was set to show maximum image contrast, using a polarizer. All lenses from M-M modules except for (e), obtained from an Intersol module.

Cross-Sectional Microscopy: Facet Tip Geometry

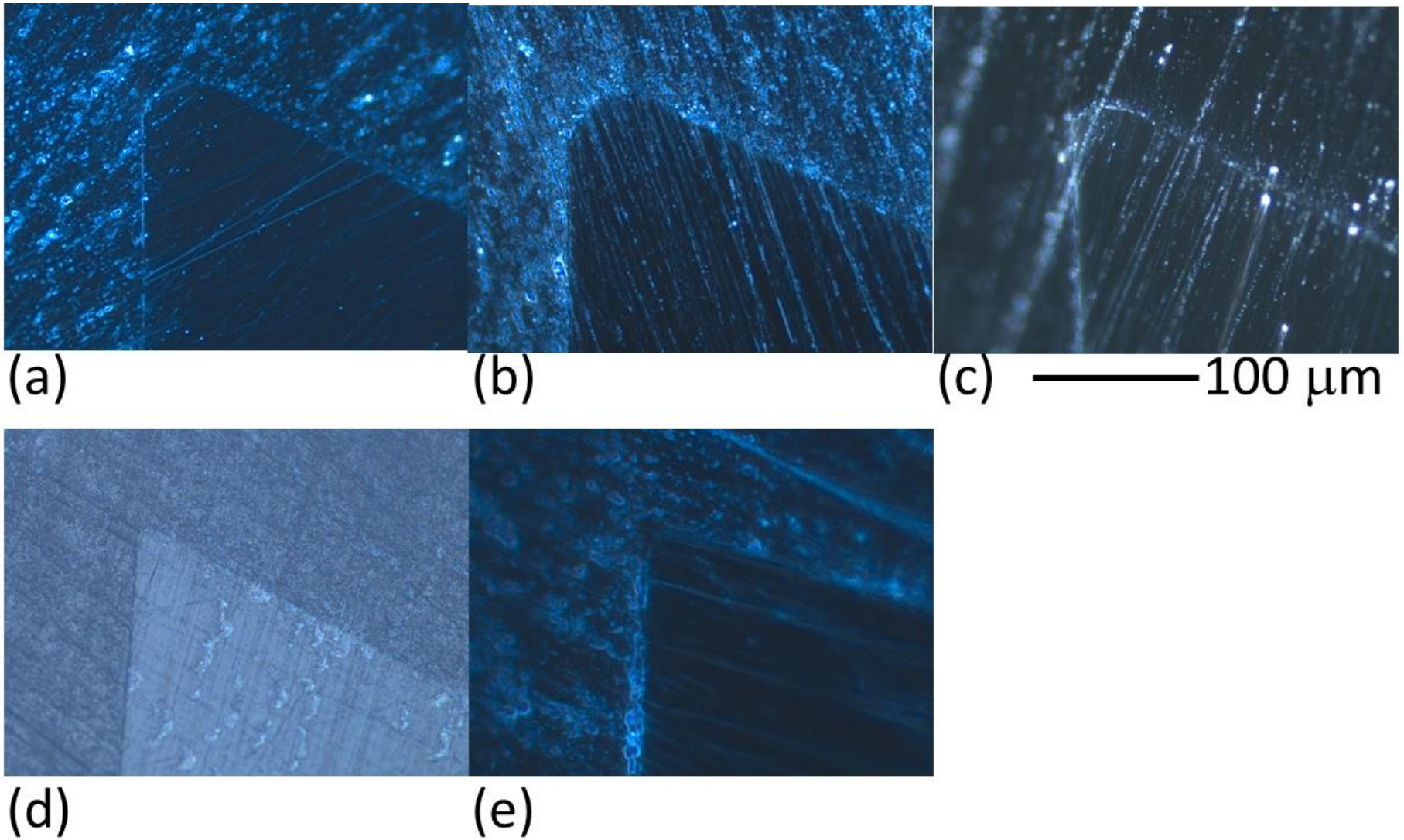

Representative micrographs from optical images of veteran and reference lenses. The images, originally obtained at 500x, are shown for: (a) NREL, warehouse; (b) KACST, reference; (c) KACST, Riyadh field 20 y; (d) APS, Phoenix field 27 y; (e) APS, Phoenix, field 22 y. The color during imaging was set to show maximum image contrast, using a polarizer. All lenses from M-M modules except for (e), obtained from an Intersol module.

Cross-Sectional Microscopy: Facet Tip Radius

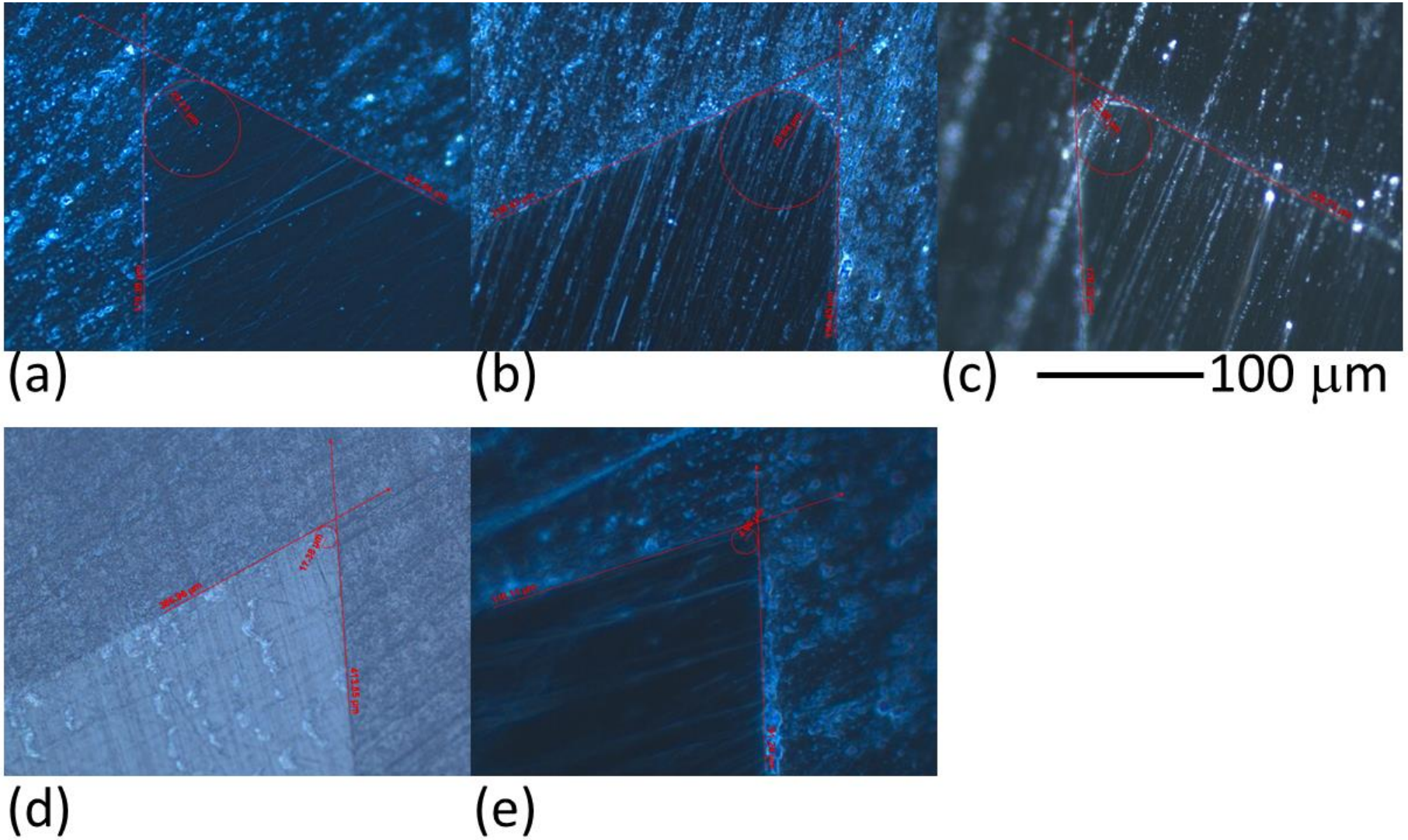

F
500x, are shown for: (a) NREL, warehouse; (b) KACST, reference; (c) KACST, Riyadh field 20 y; (d) APS, Phoenix field 27 y; (e) APS, Phoenix, field 22 y. The color during imaging was set to show maximum image contrast, using a polarizer. All lenses from M-M modules except for (e), obtained from an Intersol module.

Cross-Sectional Microscopy: Facet Valley Geometry

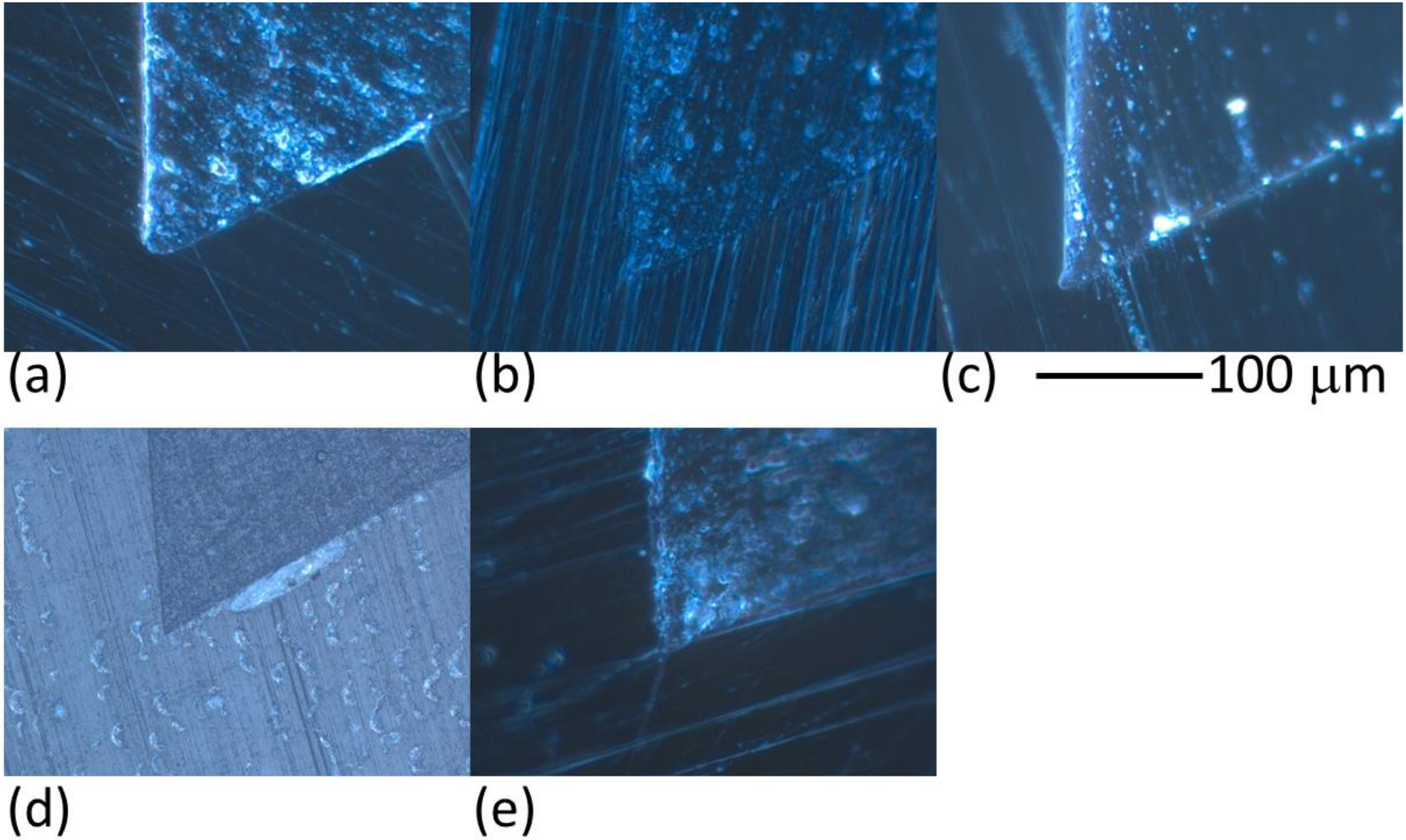

Representative micrographs from optical images of veteran and reference lenses. The images, originally obtained at 500x, are shown for: (a) NREL, warehouse; (b) KACST, reference; (c) KACST, Riyadh field 20 y; (d) APS, Phoenix field 27 y; (e) APS, Phoenix, field 22 y. The color during imaging was set to show maximum image contrast, using a polarizer. All lenses from M-M modules except for (e), obtained from an Intersol module.

Cross-Sectional Microscopy: Facet Valley Radius

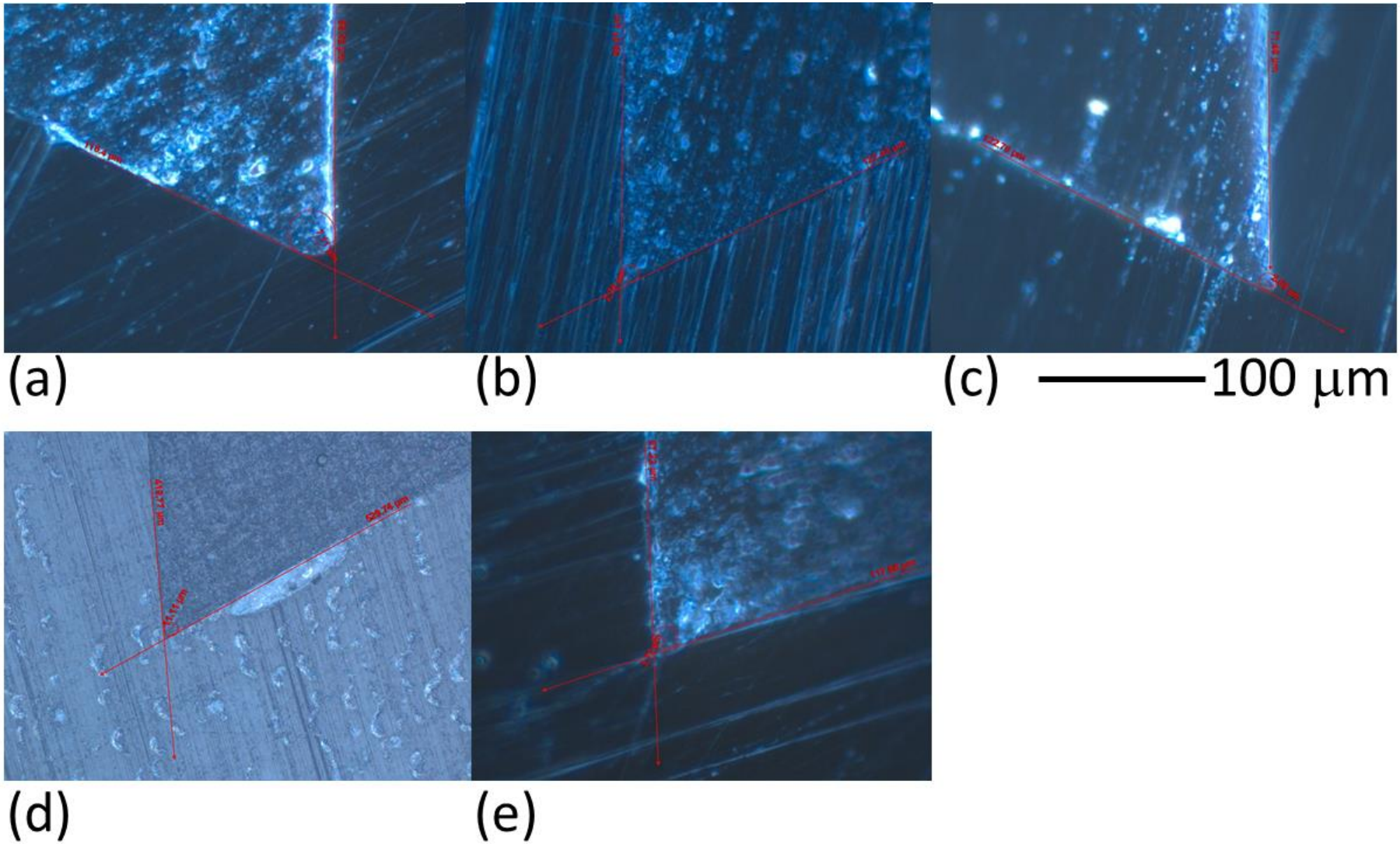

Representative micrographs from optical images of veteran and reference lenses. The images, originally obtained at 500x, are shown for: (a) NREL, warehouse; (b) KACST, reference; (c) KACST, Riyadh field 20 y; (d) APS, Phoenix field 27 y; (e) APS, Phoenix, field 22 y. The color during imaging was set to show maximum image contrast, using a polarizer. All lenses from M-M modules except for (e), obtained from an Intersol module.